

1978

Effect of random aperiodicity on threshold gain of a distributed feedback semiconductor laser

Richard William Stewart
Iowa State University

Follow this and additional works at: <https://lib.dr.iastate.edu/rtd>

 Part of the [Electrical and Electronics Commons](#)

Recommended Citation

Stewart, Richard William, "Effect of random aperiodicity on threshold gain of a distributed feedback semiconductor laser" (1978).
Retrospective Theses and Dissertations. 6594.
<https://lib.dr.iastate.edu/rtd/6594>

This Dissertation is brought to you for free and open access by the Iowa State University Capstones, Theses and Dissertations at Iowa State University Digital Repository. It has been accepted for inclusion in Retrospective Theses and Dissertations by an authorized administrator of Iowa State University Digital Repository. For more information, please contact digirep@iastate.edu.

INFORMATION TO USERS

This material was produced from a microfilm copy of the original document. While the most advanced technological means to photograph and reproduce this document have been used, the quality is heavily dependent upon the quality of the original submitted.

The following explanation of techniques is provided to help you understand markings or patterns which may appear on this reproduction.

1. The sign or "target" for pages apparently lacking from the document photographed is "Missing Page(s)". If it was possible to obtain the missing page(s) or section, they are spliced into the film along with adjacent pages. This may have necessitated cutting thru an image and duplicating adjacent pages to insure you complete continuity.
2. When an image on the film is obliterated with a large round black mark, it is an indication that the photographer suspected that the copy may have moved during exposure and thus cause a blurred image. You will find a good image of the page in the adjacent frame.
3. When a map, drawing or chart, etc., was part of the material being photographed the photographer followed a definite method in "sectioning" the material. It is customary to begin photoing at the upper left hand corner of a large sheet and to continue photoing from left to right in equal sections with a small overlap. If necessary, sectioning is continued again — beginning below the first row and continuing on until complete.
4. The majority of users indicate that the textual content is of greatest value, however, a somewhat higher quality reproduction could be made from "photographs" if essential to the understanding of the dissertation. Silver prints of "photographs" may be ordered at additional charge by writing the Order Department, giving the catalog number, title, author and specific pages you wish reproduced.
5. PLEASE NOTE: Some pages may have indistinct print. Filmed as received.

Xerox University Microfilms

300 North Zeeb Road
Ann Arbor, Michigan 48106

7904021

STEWART, RICHARD WILLIAM
EFFECT OF RANDOM APERIODICITY ON THRESHOLD
GAIN OF A DISTRIBUTED FEEDBACK SEMICONDUCTOR
LASER.

IOWA STATE UNIVERSITY, PH.D., 1978

University
Microfilms
International

300 N. ZEEB ROAD, ANN ARBOR, MI 48106

Effect of random aperiodicity on threshold gain of a
distributed feedback semiconductor laser

by

Richard William Stewart

A Dissertation Submitted to the
Graduate Faculty in Partial Fulfillment of
The Requirements for the Degree of
DOCTOR OF PHILOSOPHY

Major: Electrical Engineering

Approved:

Signature was redacted for privacy.

In Charge of Major Work

Signature was redacted for privacy.

~~For the~~ Major Department

Signature was redacted for privacy.

For the ~~Graduate~~ College

Iowa State University
Ames, Iowa

1978

TABLE OF CONTENTS

	Page
I. INTRODUCTION	1
A. Statement of the Problem	1
B. Review of Semiconductor Laser	14
C. Effect of Aperiodic Media	24
II. DERIVATION OF PERTURBED THRESHOLD CONDITION	28
A. Approximate Solutions for the Unperturbed Periodic Structure	29
B. Propagation in a Perturbed Medium	39
C. Threshold Condition for Perturbed Media	46
III. EFFECT OF PERTURBATION OF PERIODIC MEDIUM ON THE THRESHOLD CONDITION	58
A. Approximate Expression for the Perturbed Gain Parameters and Phase Parameters	58
IV. DISCUSSION OF RESULTS	72
V. CONCLUDING REMARKS	80
A. Suggestion for Further Studies	83
VI. REFERENCES	85
VII. ACKNOWLEDGMENTS	92
VIII. APPENDIX	93

LIST OF FIGURES

	Page
Figure 1. Examples of periodic waveguide for thin-film lasers, (a) structure utilizing periodic variation in thickness of top dielectric layer, (b) structure utilizing periodic in thickness of film	6
Figure 2. The basic periodic waveguide models and the form of assumed wave solution, (a) coupled mode formalism, (b) truncated Floquet-Bloch formalism $P = \Gamma + iK_B$, $\Gamma = G - ik$	8
Figure 3. The periodic variation of $k_z(z)$ in the periodic waveguide	11
Figure 4. Diagram showing reflection and transmission at the boundaries between uniform and periodic media. The reflected and transmitted fields U_R and U_T can be expressed in terms of incident field by matching the boundary conditions	13
Figure 5. Diagram showing reflection and transmission at the boundaries between uniform and perturbed periodic regions	48
Figure 6. The variation of the gain parameters x , x_0 and phase parameters y , y_0 , with the coupling parameter τ for a perfectly periodic structure $x = (G_0 L)$, $x_0 = (g_0 L)$, $y = (\delta_e L)$, $y_0 = (\delta L)$, $\tau = (\kappa L)$	55
Figure 7. The variation of the gain parameter x_0 with the coupling parameter τ for different values of the perturbation parameter ρ_0	67
Figure 8. The variation of the phase parameter y_0 with the coupling parameter τ for different values of the perturbation parameter ρ_0	68
Figure 9. The variation of the perturbed effective gain parameter \bar{x} with the coupling parameter τ for different values of the perturbation parameter ρ_0	69

	Page
Figure 10. The variation of the perturbed effective phase parameter \bar{y} with the coupling parameter τ for different value of the perturbation parameter ρ_0	70
Figure 11. The variation of the relative change in the effective gain parameter; $\Delta x/x$ with the coupling parameter τ for different values of the perturbation parameter ρ_0	76
Figure 12. The variation of the relative change in the effective phase parameter; $\Delta y/y$ with the coupling parameter τ for different values of the perturbation parameter ρ_0	77

I. INTRODUCTION

A. Statement of the Problem

Since first developed by Kogelnik and Shank (1) the distributed feedback laser (DFB) has received wide-spread attention as a device suitable for use in integrated optical circuits (2-16). The distributed feedback structure employed in the thin-film DFB device is capable of providing compact, low loss optical cavities for thin-film lasers which allows longitudinal mode control and frequency selection. Essentially these are periodic waveguide structures superimposed on the gain medium. The feedback mechanism is backward Bragg scattering.

One of the characteristic properties of periodic structures is the distributed reflections or feedback that occur in well-specified frequency bands near the Bragg frequencies. These Bragg frequencies are defined by $\lambda = 2\Lambda/v$, where λ is the corresponding wavelength of the propagating wave, Λ is the spatial period of the structure, and N is a positive integer that corresponds to the Bragg order. The precise location of oscillation wavelengths of a thin-film DBF is also determined by the Bragg wavelength, which in turn is determined by the period Λ , and film thickness.

The distributed feedback laser, indeed any electro-optical device depending on Bragg scattering for its operation,

requires a periodic structure. The production of a DBF device requires fabrication of a periodic structure with a fundamental period on the order of an optical wavelength. Such a finely structured grating challenges current fabrication techniques (17-22), and may well contain flaws which must result in less than perfect periodicity and distortion. In evaluating the potential operation of DFB lasers, inaccuracy in controlling the periodicity must be taken into account.

It appears that the effect of distortion in periodicity of the structure of the active medium in a DFB laser has not been studied and reported in the literature. Therefore, it is the objective of this study to investigate the effect of a random aperiodicity or deviation from perfect periodicity on the threshold gain and frequency of a distributed feedback laser. In other words, we shall examine the effect of the flaws in the fabrication of the periodic structure on the threshold gain required to achieve lasing in the structure and on the frequency at which lasing occurs.

Like many techniques, the development of fabrication techniques for electro-optical periodic structures has been evolutionary. Techniques first used for fabrication of planar silicon integrated circuits (17) have blended with classical and holographic optical techniques to produce useful

structures (18-22). The construction of a periodic structure is fundamentally a two-step procedure (22). First the desired pattern is produced on a mask. The mask is superimposed over the base material or substrate leaving appropriate portions shielded or exposed. Second, the exposed material is altered either in physical profile by etching or in electrical properties by diffusion or deposition of a dissimilar material.

Both these processes have inherent inaccuracies which result in deviations from the desired ideal structure. The magnitude and nature of these deviations depends on the particular process. Several variations exist. First, the mask is usually a radiation sensitive polymer which is exposed to radiation of the desired pattern. The radiation pattern may be generated directly or by yet another mask. Each intermediate mask may introduce distortion from scale changes and optical imperfections. Radiation sources are usually optical but may be x-ray or electron beam. Direct pattern generation may be by externally driven control of an electron beam. Resolution and distortion are defined by the precision with which the beam may be focused, by precision in the direction and location controls and by diffraction and backscatter of the beam. Alternatively, a pattern may be generated by superposition of two or more coherent sources. Distortion arises from source incoherence and departure from an optically flat substrate or from plane wave incidence.

Once the mask has been formed, the exposed material must be altered. The most common process is chemical etching. Unfortunately, etching may undercut the mask if deep grooves are etched. Ion beam etching provides reasonably clear definition but requires a thick mask to prevent faceting or undercutting. Diffusion of impurities into the exposed substrate gives indefinite boundaries and fails to induce significant optical variation. Typical total distortion for a structure produced under laboratory conditions is 10^{-4} to 10^{-5} for a holographically prepared mask and ion beam etching (22).

To obtain a good understanding of the principle of operation of the DFB laser, we must have a proper understanding of phenomenon of wave propagation in the periodic structure. The operation of the distributed feedback DFB laser in the thin-film semiconductor configuration has been interpreted and explained in terms of two complementary models: (a) coupled-mode formalism (2, 23-25) and (b) Floquet-Bloch modes approach (3, 26, 27).

An example of a periodic waveguide for a thin-film laser is shown in Figure 1. The wave propagation in the periodic structure as shown in Figure 1 can be characterized by

$$k_x^2 + k_z^2 = k_0^2 n_f^2, \quad (1.1)$$

where k_x and k_z are the transverse and the longitudinal wave numbers, and k_0 denotes the free space wave number. n_f is the film index of refraction. Any change in k_x will result in a corresponding change in k_z thereby generating a reflected wave. In a DFB laser the spatial variation of d and W (in Figure 1) is made periodic so that the reflected wave generated by a spatially varying k_z can maintain the proper phase relation for constructive feedback. Wave propagation in the waveguide involves both the coordinates x and z and hence is a two-dimensional problem. This two dimensional problem has been analyzed by Wang (28), Wang and Shen (29) and DeWames and Hall (30).

Under the assumption of small perturbations one-dimensional analysis is applicable (3). In other words the problem can be described by the solution of a one-dimensional wave equation which must be satisfied by the electric field intensity of the optical wave in the active medium:

$$\frac{d^2 E}{dz^2} - \gamma^2 E = 0, \quad (1.2)$$

where $\gamma = g - ik_z(z)$ is the complex propagation. Here g and $k_z(z)$ denote the gain constant and the phase constant respectively.

In the coupled mode approach one chooses to expand the field in the periodic waveguide in terms of the modes of

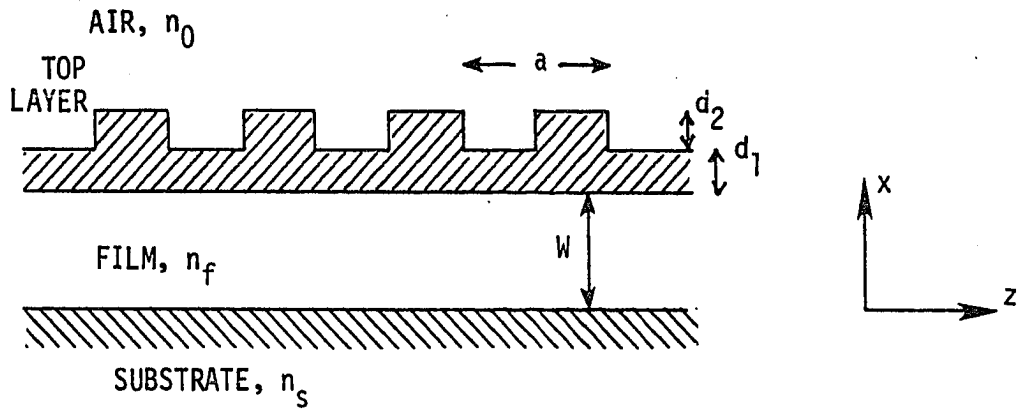


Fig. (a)

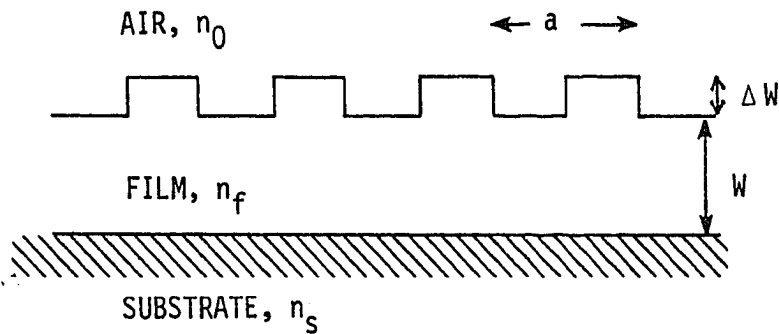


Fig. (b)

Figure 1. Examples of periodic waveguide for thin-film lasers
 (a) Structure utilizing periodic variation in thickness of top dielectric layer
 (b) Structure utilizing periodic in thickness of film

the unperturbed uniform wave-guide which constitute an orthonormal set (23). When one substitutes the assumed solution into the Maxwell's equation and limits the expansion to the two modes which are Bragg-coupled ($|\beta| = K_B$, see Figure 2 for detail), the result is the coupled-mode equation (24).

$$\frac{dB}{dz} = -i\kappa A \exp[-i2(\beta - K_B + ig_0)z] \quad (1.3a)$$

$$\frac{dA}{dz} = i\kappa B \exp[i2(\beta - K_B + ig_0)z], \quad (1.3b)$$

whose solutions are given in reference (2) for the case of a DFB laser. Here β and g_0 , are the phase constant and the gain constant, respectively, and $K_B = \frac{\pi}{a}$ is the Bragg wave number and "a" denotes the spatial period. κ is the coupling coefficient determined by the modulation of the structure. A and B represent the amplitudes of forward and backward wave (see Figure 2a).

Kogelnik and Shank (2) describe the field as coupled forward and backward waves, which are described by the following coupled differential equations:

$$-\frac{dR}{dz} + (g - i\delta)R = i\kappa S \quad (1.4a)$$

$$\frac{dS}{dz} + (g - i\delta)S = i\kappa R, \quad (1.4b)$$

where $R(z)$ and $S(z)$ are the forward and backward wave components of electric field intensity, and δ denotes the

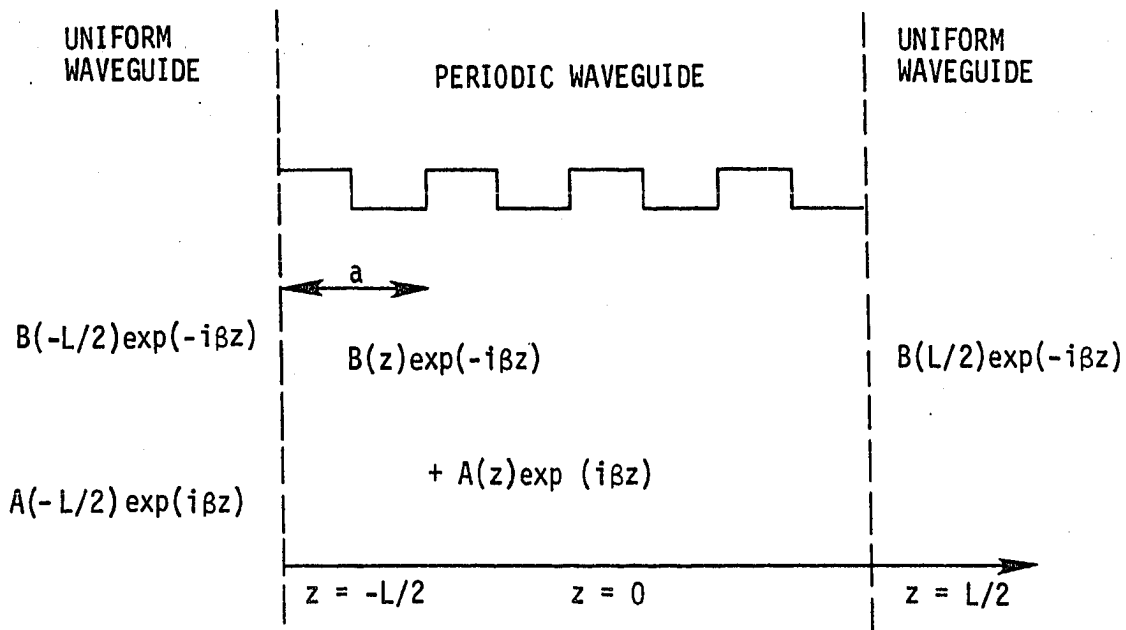


Fig. (a)

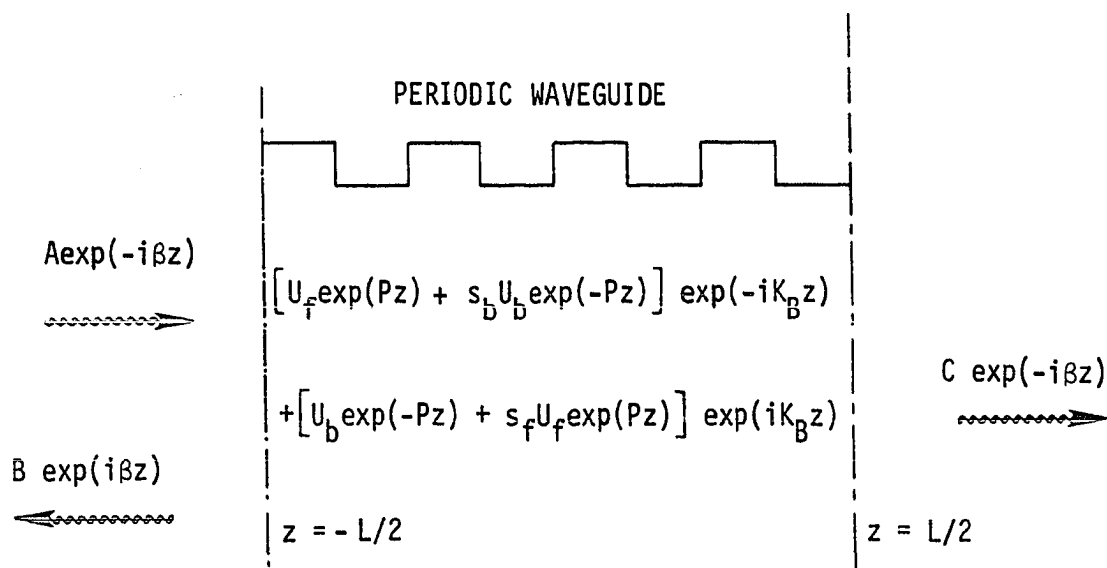


Fig. (b)

Figure 2. The basic periodic waveguide models and the form of assumed wave solution. (a) coupled mode formalism (b) truncated Floquet-Bloch formalism $P = \Gamma + iK_B$, $\Gamma = G - iK$.

amount of detuning from the Bragg condition.

In dealing with the coupled wave phenomenon usually one considers two waves or modes (R and S) of a guiding structure which propagate freely and uncoupled as long as the structure is not perturbed. A perturbation of the original structure, e.g., an induced change of the refractive index of the film guide, will lead to a coupling of two waves and an exchange of energy between them.

An important requirement for a significant interaction is the synchronism or "phase-matching" between the two coupled waves, which in the simplest case is the requirement for the equality $\beta_R = \beta_S$ of the phase constants β_R and β_S of the two waves. The scattering of light by a periodic structure can be viewed as a coupled wave process.

The imposition of the boundary condition $S(\frac{L}{2}) = R(-\frac{L}{2}) = 0$ results in a longitudinal mode spectrum for each transverse wave guide mode similar to that existing in Fabry-Perot resonator of the same length (see Figure 2a).

On the other hand, in the truncated Floquet-Bloch formalism of Cordero and Wang (3, 26, 27), the solution is in the form of four waves (two fundamental components and two associated space harmonics) as shown in Figure 2b.

According to Floquet's theorem, Equation (1.2) has a solution of the form:

$$E(z) = A\phi_1(z) \exp(\Gamma_0 z) + B\phi_2(z) \exp(-\Gamma_0 z) \quad (1.5)$$

where $\phi(z) = \phi(z+a)$ is a periodic function of period a . Since $\phi(z)$ repeats itself from period to period, the long range behavior of $E(z)$ is governed by $\exp(+\Gamma_0 z)$ in so far as the amplitude of the wave is concerned.

To find the form of $\phi(z)$ and the value of Γ_0 , the dependence of $\gamma(z)$ on z must be specified. Although $k_z(z)$ in Equation (1,2) can be any periodic function of z , the rectangular variation shown in Figure 3 is typical. Wang (3) uses this rectangular variation to study representative behavior of the propagation constant Γ_0 near the Bragg frequency, ω_0 . The propagation constant $\Gamma_0 = G_0 - iK_0$ in the periodic medium is complex with G_0 representing the effective gain constant and K_0 representing the effective phase constant. The Bragg frequency, ω_0 , is the frequency at which the average phase propagation constant β equals the Bragg wave number π/a . The distributed feedback coefficient, κ , is the average reflection per unit length. For the structure shown in Figure 3, $\beta = (\beta_1 + \beta_2)/2$, $a = a_1 + a_2$ and $\kappa = (\beta_2 - \beta_1)/\pi$. It should be noted that near ω_0 , the effective propagation constant Γ_0 in the periodic waveguide differs considerably from γ_0 , the propagation constant in a corresponding uniform waveguide. The thin-film device under discussion can be characterized by the relationship of the

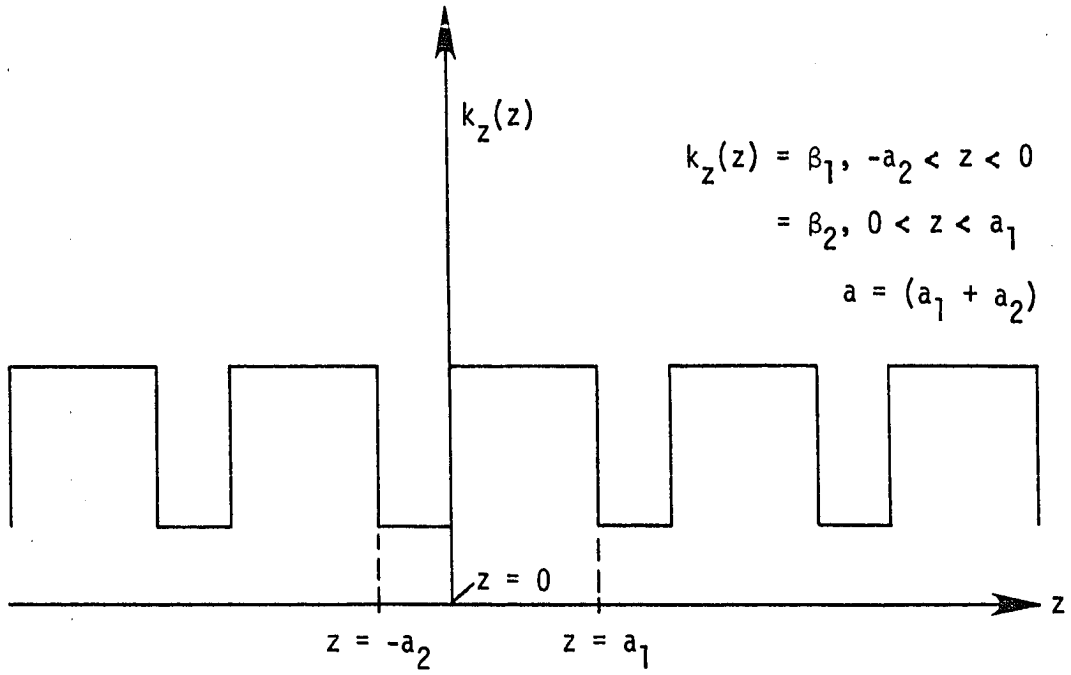


Figure 3. The periodic variation of $k_z(z)$ in the periodic waveguide.

reflected and transmitted wave U_R and U_T to the incident wave (see Figure 4).

Using the field expression $E = U \exp[+i\beta z]$ for the wave in the uniform waveguide and $E = U_B f(z) \exp[+\Gamma_0 z]$ for the two Bloch waves in the periodic waveguide and applying the continuity of tangential electric field intensity \vec{E} and magnetic field intensity \vec{H} at the two boundaries, Wang (3) obtained the threshold condition of thin-film Bragg laser.

It should be pointed out that the comparison of the method of the coupled-mode formalism with the method of Floquet-Bloch wave formalism shows that near the Bragg regime, the two methods yield the same dispersion relationship. Yariv and Gover (31) recently have shown that the truncated Floquet-Bloch approach is formally equivalent to that of the coupled-modes. The difference in the form of solution assumed in the two approaches is shown in Figure (2a) and Figure (2b). The main attraction of the coupled-wave analysis is the simplicity. However, many details that are missing in the coupled-mode analysis could prove important in realizing the full potential of DFB laser. Consequently, we shall use the truncated Floquet-Bloch approach in the present study of the effect on the threshold condition of the aperiodicity in the perturbed periodic structure. The method of analysis, used by Wang (3), for studying the perfectly periodic structure is to be extended to include the

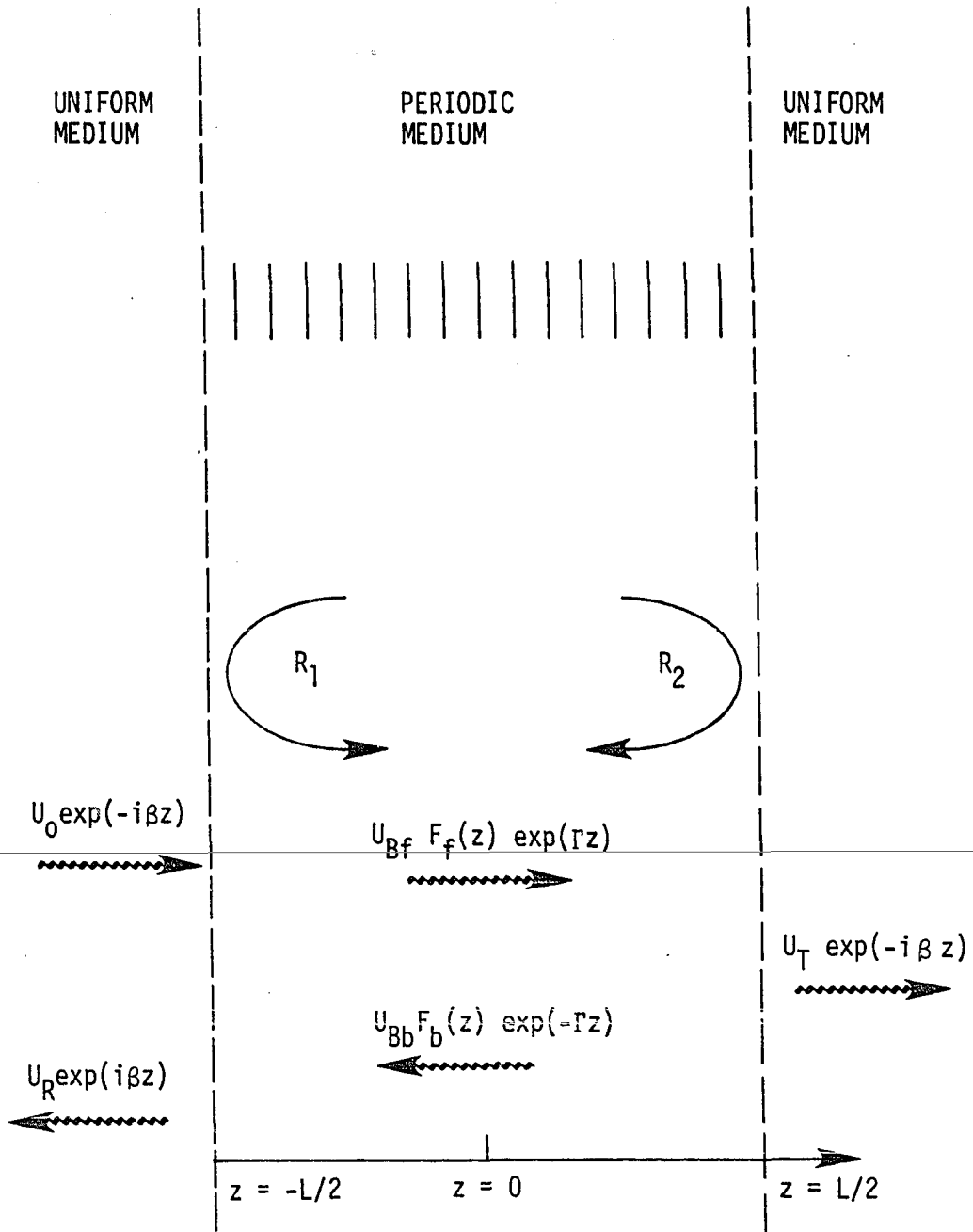


Figure 4. Diagram showing reflection and transmission at the boundaries between uniform and periodic media. The reflected and transmitted fields U_R and U_T can be expressed in terms of incident field by matching the boundary conditions.

effect of distortion in the periodicity. The perturbed threshold condition is derived in Section II, and the effect of the perturbation on the threshold condition is investigated in Section III.

B. Review of Semiconductor Laser

As is well-known, a quantum ensemble of two or more energy states may interact with an incident electro-magnetic wave of the proper energy or frequency (32-36). For simplicity, consider only two energy levels separated by $\hbar\omega$. Two events may occur. First, an incident photon may, if sufficiently energetic, be absorbed and excite a member of the ensemble from the lower energy state to the higher. Second, the incident photon may stimulate the transition of a member of the ensemble from the upper state to the lower state. This transition emits a new photon of energy $\hbar\omega$ which is in phase with the initially incident photon. Additionally, spontaneous emission of a photon by unstimulated transition from higher to lower states occurs at a rate independent of stimulated emissions.

The probability of either stimulated transition may be calculated using time dependent perturbation techniques (33). In general, we find that the probability of an ensemble member in a lower state absorbing a photon is the same as the probability of an ensemble member in the upper state emitting a photon. This probability reaches its maximum when the incident photon has energy at or near $\hbar\omega$. Finally, the probability of either

transition occurring is proportional to the incident field intensity.

These observations define the requirement for lasing. First, predominance of stimulated emission over absorption requires a surplus population of ensemble members in the higher energy state. In a realizable system stimulated emission must also dominate all loss mechanisms. Second, predominance of stimulated emission over spontaneous emission requires a threshold incident field. Finally, the field must have a frequency at or near the quantum transition frequency.

While the preceding discussion applies directly to ensembles of discrete quantum oscillators, the quantum characteristics of semiconductors differ in several respects. The periodic nature of the crystal modifies the Schrodinger solution for free electrons so the electrons form an interactive ensemble rather than isolated oscillators. The periodicity creates ranges or bands of allowed energies separated by bands of disallowed or forbidden energies. Transitions of electrons between states separated by a band gap form the basis for lasing (35-40).

The relative probability of an electron occupying a particular equilibrium energy state, is given by Fermi-Dirac distribution,

$$f^{-1}(\epsilon) = 1 + \exp[(\epsilon - F)/k_B T] \quad (1.6)$$

where

F is the Fermi level,

k_B is Boltzman's constant, and

T is the temperature in degrees Kelvin.

To calculate the requirement for stimulated emission dominating absorption, let

f_C be the probability an electron occupies a state in the upper band, and

f_V be the probability an electron occupies a state in the lower band.

Stimulated emission across the band gap $E_C - E_V$ requires an occupied state at E_C and an unoccupied state at E_V . Similarly, absorption requires an occupied state at E_V and an empty state at E_C . Since the transition rates for absorption and emission are equal, the dominance of either process depends entirely on the relative probability of the preceding conditions. Hence, emission will dominate absorption if

$$f_C(1-f_V) > f_V(1-f_C) \quad (1.7a)$$

or

$$f_C > f_V \quad (1.7b)$$

Suppose the electrons in each band are in thermal equilibrium. Then, if electrons are injected into the upper band or removed from the lower band, the probability of an electron occupying a state E_2 in the upper band or E_1 in the lower band is

$$f_C^{-1} = 1 + \exp[(E_2 - F_C)/k_B T] \quad (1.8a)$$

$$f_V^{-1} = 1 + \exp[(E_1 - F_V)/k_B T] \quad (1.8b)$$

where F_V is the quasi-Fermi level in the valence band, and F_C is the quasi-Fermi level in the conduction band.

Consequently, the requirement for net emission is

$$F_C - F_V > E_2 - E_1 \quad (1.9a)$$

or

$$F_C - F_V > \hbar\omega. \quad (1.9b)$$

This requires that the semiconductor be degenerate and, if a p-n junction is used to provide the population inversion, the forward bias must be greater than $\hbar\omega$.

The population inversion may be created in several ways, some more efficient than others. In conventional lasers, either an intense incoherent optical source or an arc discharge creates a surplus population in the upper state (33). Arc discharge excitation seems inappropriate for a semiconductor, although avalanche breakdown excitation received some early attention (41). Optical excitation may be used, but requires a monochromatic source, i.e., another laser. External efficiency is not high. Furthermore, since the absorption rate is quite high, only a small volume of material is excited (33).

Fortunately, the well-studied p-n junction under forward

bias injects a surplus of conduction electrons and/or removes valence electrons, thus creating an effective population surplus. The forward biased junction has a relatively low impedance, allowing high current flow and hence a strongly inverted population at low voltages.

Since first suggested in 1963 (39), p-n junction lasers have been fabricated in many configurations and materials. However, for semiconductors with band gaps corresponding to optical frequencies, the Einstein coefficient relating the ratio of spontaneous to stimulated emission is rather high. Very high radiation densities and large population inversions are thus needed to achieve lasing. Most applications where coherence is not an absolute requirement therefore use the simple p-n junction as a source of relatively monochromatic but incoherent light (37).

Thus conventional p-n semiconductor-junctions have failed to meet early expectations of widespread usefulness. For example, in the homojunctions the excessively high threshold currents at room temperature and the requirement for a cryogenic environment for continuous operation severely limit this device's application as a coherent source.

However, as first proposed in 1963 (42), performance of an injection laser may be improved by surrounding the active junction region with a material of higher energy band gap. Two principal advantages accrue. First, the wider band

gap material with its lower index of refraction, defines a dielectric optical waveguide and confines the electric field to approximately the region of the junction. Second, the wider gap itself provides a potential barrier and retards the diffusion of minority injected carriers away from the active junction area. The net result is both a higher field intensity and an enhanced concentration of minority carriers, both of which favor a higher rate of stimulated emission. Panish (43, 44) gives two excellent reviews of heterostructure laser properties.

Injection devices consisting of two or more materials with distinct band gaps are called heterostructures. While in principle, heterostructures may consist of two simple semiconductors such as silicon and germanium, both materials have indirect band gaps and are hence unsuited for injection lasers. The more usual combination consists of modified III-V compounds, typically gallium arsenide. Stoichiometric substitution of an element with similar valence for a fraction of either the III or V component alters the band gap of the compound semiconductor. For example, Casey and Panish (45) show that the band gap of $\text{Ga}_{1-x}\text{Al}_x\text{As}$ increases with x . Similarly, Alferov (46) reports that the band gap of $\text{GaAl}_{1-x}\text{Sb}_x$ increases with x . In both compounds, the

index of refraction decreases as the band gap widens.

Mixing dissimilar III or V valent atoms with the lattice often alters the lattice parameters. For example, due to the different effective radii of Sb and As, the lattice parameters of $GaAs_{1-x}Sb_x$ vary significantly with x (44). As a consequence, the junction boundary of a $GaAl_{1-x}Sb$ -GaAl heterojunction suffers severe crystal discontinuities. These discontinuities create many nonradiative recombination centers which trap minority carriers otherwise available for stimulated emission. The reduction in effective population inversion usually precludes lasing at reasonable injection currents. On the other hand, the lattice parameters of $Ga_{1-x}Al_xAs$ vary only slightly with x . The crystal discontinuities at the boundary of a $Ga_{1-x}Al_xAs$ -GaAs junction remain limited. The number of nonradiative recombination centers is reduced and injection of minority carriers may yield a reasonable population inversion. Consequentially, the $Ga_{1-x}Al_xAs$ -GaAs heterojunction provides the base for most heterostructure lasers.

Unlike gas or crystalline ruby lasers, semiconductor lasers require optical waveguiding along the resonance path. This confinement of the field pattern increases the field intensity in the active region. The more intense field enhances stimulated emission and gain coupling of the field

and media (47, 48).

Dielectric waveguiding typically occurs in a three layer structure. If the central layer's index of refraction exceeds the indices of the other two layers, the propagation velocity of the central layer is lowest. Hence, a wavefront of constant phase propagating parallel the slab boundaries must be concave in the direction of propagation, thus focusing or confining the field.

Of course, many modes may propagate in such a structure. According to Panish et al. (49) and Ikegami (50) transverse electric modes usually dominate since these modes have a larger reflectivity at the cavity mirrors.

Knowledge of exact propagation and field confinement for the dielectric slab waveguide requires solution of the wave equation for the particular structure. Standard techniques involving proper boundary values, separation of variables, eigenvalues and functions apply. Detailed solution methods and results are given by numerous authors including Born and Wolf (51), Harrington (52), and Marcuse (53),

In the heterostructure lasers, the dissimilar indices of refraction arise from two causes. First, the outer $\text{Al}_x\text{Ga}_{1-x}\text{As}$ layer has a lower intrinsic index of refraction with an increased band gap. Interestingly, Moss (54) states an empirical rule for the correlation of semiconductor band gap as $n^4 E_g = 77$.

Pankove (38) notes an effect which enhances waveguiding when a wider gap semiconductor surrounds the active region. By modifying the Kramers-Kroneg relation for frequency dependent indices of refraction, the following expression evolves.

$$n(E) - 1 = \frac{ch}{2\pi^2} P \int_0^{\infty} \frac{\alpha(E')}{(E')^2 - E^2} dE' \quad (1.10)$$

where

$E = h\nu$ is the photon energy

P = Cauchy principal value

α = absorption coefficient

n = index of refraction

The absorption coefficient remains small for energies less than the band gap. Hence, photons generated by band to band recombination in the lower gap material will encounter the lower range of the higher gap material's index of refraction.

Current flow and hence minority injection in heterostructures closely resembles the mechanism found in a Schottky barrier (38, 55). The forward current density increases exponentially with applied voltage so that the junction impedance remains well below ohmic contributions from bulk material and contact resistivity. Thus, like the conven-

tional diode, the heterojunction allows injection of a large concentration of minority carriers into the active recombination region with a low applied voltage. Additionally, the band structure of a Ppn or Nnp junction effectively confines the injected minority carriers to a relatively narrow region (49, 56, 57).

The combination of dielectric waveguiding and minority carrier confinement increases the efficiency of the heterostructure, so that both continuous and room temperature lasing are now commonplace (43, 44, 58-60). Consequently, the heterostructure has virtually replaced the homostructure for semiconductor lasers.

As noted earlier, population inversion is of itself insufficient to achieve lasing. While an adequate inversion provides for dominance of emission over absorption and other loss mechanisms, stimulated emission must also dominate spontaneous emission. Again the frequency dependence of the Einstein coefficient shows that lasing at optical frequencies requires an intense radiation density. This radiation density is usually provided by containing the active medium within a structure having a resonance frequency at the quantum transition frequency of the medium. Although the choice of resonant structures is virtually unlimited, the most widely used structure remains the Fabry-Perot cavity consisting of two parallel, or in some variations slightly concave (33)

reflectors. The Fabry-Perot cavity resonates at frequencies where an integral number of wavelengths separate the reflectors. Since at optical frequencies, a sizeable number of frequencies meet this criterion, the quantum transition frequency defines the operating resonance.

In semiconductor lasers, the transition frequency is broader than in ruby or gas lasers and minor variations in structure geometry and material properties lead to significant variations of operating frequencies among lasers, even those fabricated from the same chip (35). Such variations may be undesirable for communications applications. Alternatively, a periodic structure may provide the resonance requirements and define a less ambiguous frequency of operation. Additionally, a periodic structure does not need cleaved reflecting planes at the ends of the structure and is therefore more easily incorporated into a larger integrated circuit. Thus the distributed feedback laser has been developed.

C. Effect of Aperiodic Media

The analysis of waves propagating through a randomly disturbed medium, occupies a sizable volume of literature (61-63). Ishimaru (63) provides a comprehensive review and extensive bibliography.

Both the disciplines of RF communication and radio

astronomy include well-motivated studies of propagation in random media (64, 65). In fact an important communication technique, tropospheric scatter, relies entirely on the presence of atmospheric inhomogeneity for its operation (66). Random inhomogeneities are usually less benign, generally increasing noise and fading in radio links. Radio astronomers find that atmospheric and interstellar medium perturbations muddy the already darkened window to the universe.

Most modern methods for treating random inhomogeneities have several common features: First, a characterization of the medium with a uniform, small, zero mean perturbation. Second, a description of the perturbations by their spectral density or autocorrelation function. Third, an attempt to identify the expected deviations from the unperturbed phase and amplitude some distance from the source. Coherent phase contributions such as would be found in a periodic medium appear as singularities and are avoided with due trepidation.

The preceding claim overstates the difficulties of treating coherent phase contributions. Several techniques evolving from x-ray crystallography use scattering patterns to elicit information about the spatial distribution of scattering centers or inhomogeneities within a medium. However, these techniques generally apply to far-field distributions for weak scattering of a uniform plane wave

(67, 68). An interesting treatment of scattering from a perturbed periodic structure ascribed to Debye is shown below (69).

Consider an ensemble of M scattering centers of scattering intensity f_j at locations \vec{r}_j . The total scattered amplitude at exterior location \vec{r}' is given by

$$A_0(\vec{r}') = \sum_{j=1}^M f_j \exp(2\pi i \vec{r}' \cdot \vec{r}_j) \quad (1.11)$$

Suppose each of these scattering centers is displaced from its equilibrium position by an amount Δr_j . Then the total scattering amplitude now becomes:

$$\begin{aligned} A(\vec{r}') &= \sum_{j=1}^M f_j \exp[2\pi i \vec{r}' \cdot (\vec{r}_j + \Delta \vec{r}_j)] \\ &= \sum_{j=1}^M \exp(2\pi i \vec{r}' \cdot \Delta \vec{r}_j) f_j \exp(2\pi i \vec{r}' \cdot \vec{r}_j) \end{aligned} \quad (1.12)$$

Suppose the Δr_j 's are independently random. Then we may exchange expectation and summation to obtain:

$$\epsilon\{A(\vec{r}')\} = \sum_{j=1}^M \epsilon\{\exp(2\pi i \vec{r}' \cdot \Delta \vec{r}_j)\} f_j \exp(2\pi i \vec{r}' \cdot \vec{r}_j) \quad (1.13)$$

If the Δr_j 's have equivalent statistics, then

$$\begin{aligned}
\varepsilon\{A(r')\} &= \varepsilon\{\exp(2\pi i \vec{r}' \cdot \Delta \vec{r})\} A_0(\vec{r}') \\
&\approx \varepsilon\{1 + (2\pi i \vec{r}' \cdot \Delta \vec{r}) - \frac{1}{2}(2\pi \vec{r}' \cdot \Delta \vec{r})^2 \dots\} A_0(r')
\end{aligned}
\tag{1.14}$$

Which, for zero mean Δr gives

$$\varepsilon\{A(\vec{r}')\} = 1 - 2\pi^2 \varepsilon\{(\vec{r}' \cdot \Delta \vec{r})^2\}
\tag{1.15}$$

We might therefore believe that similar perturbations of the periodic structure of a distributed feedback laser would decrease the effective coherent scattering and increase the threshold gain required for lasing.

II. DERIVATION OF PERTURBED THRESHOLD CONDITION

In this section we derive an equation relating the threshold gain and resonance frequency for lasing of a distributed feedback laser whose periodic structure is corrupted by a small zero mean random perturbation. The analysis contains three subsections.

First, we solve the one-dimensional wave equation for a perfectly periodic medium. After briefly considering the Floquet form and properties of propagation in periodic media and alternative methods of solution, we choose a model in which the electric field and the propagation constant in the periodic medium are both expandable as Fourier series. Since the frequency of operation lies very close to the Bragg frequency, only lowest order terms have a significant interaction and truncation of the complete Fourier series gives an approximate solution for the Floquet periodic functions and Floquet exponentials.

Next we modify the Floquet form for a medium slightly perturbed by the addition of a zero mean random variable whose spatial frequency spectrum is primarily well-below that of the unperturbed medium. The modified Floquet form retains the same periodic functions, but the Floquet exponential exhibits a shift due to the perturbing term.

Finally, the modified Floquet form enables calcula-

tion of effective reflection coefficients at the structure boundaries and calculation of the net phase and gain propagation through the structure. These properties then provide a derivation of the threshold conditions for lasing in the perturbed structure.

A. Approximate Solutions for the Unperturbed Periodic Structure

We shall develop a dispersion relation and a solution for the electric field in a periodic dielectric waveguide as found in a heterojunction or double heterojunction semiconductor laser. Assuming first that the frequency of operation is above the cut-off for the waveguide, and that the periodic perturbations are small, then the propagation may be reasonably modelled by the one-dimensional wave equation (2, 3, 70),

$$\frac{d^2 E}{dz^2} - \gamma_0^2 E = 0 \quad (2.1)$$

where the complex propagation constant $\gamma_0(z)$ is given by

$$\gamma_0(z) = g_0 - ik_0(z) \quad (2.2a)$$

and

$$k_0(z) = \bar{k} + k_1(z) \quad (2.2b)$$

$k_1(z)$ has zero mean and is periodic with spatial frequency $2K_B$

g_0 is the gain per unit length, and

E is the complex amplitude of electric field with angular frequency ω .

Our assumptions here are that

$$k_1/\bar{k} \ll 1 \quad (2.3a)$$

$$g_0 \ll K_B . \quad (2.3b)$$

In other words, the periodic disturbance is relatively small and the gain per wavelength is very small.

As is well-known the general solution of Equation (2.1) is given by the Floquet form (3, 70)

$$E(z) = A\phi(z) \exp[\Gamma_0 z] + B\psi(z) \exp[-\Gamma_0 z], \quad (2.4)$$

where $\phi(z)$ and $\psi(z)$ have the periodicity $2K_B$ of the structure and the propagation constant in the perfectly periodic structure $\Gamma_0 = (G_0 - iK_0)$ is generally complex. The subscript 0 is used to emphasize that a perfectly periodic medium is being considered. Once the functional form of $k_1(z)$ is specified, then one of several methods (3, 70, 71) may be used to solve for Γ_0 , ϕ and ψ .

We choose to use the Fourier expansion technique similar to that used by Wang (3) to obtain approximate solutions for Γ_0 , $\psi(z)$ and $\phi(z)$. Since device operation is at or near the Bragg frequency, only the lowest order modes will

contribute significantly.

First examining γ_0 , we find

$$\gamma_0^2 = [g_0 - i(\bar{k} + k_1)]^2 \quad (2.5)$$

can be approximated by

$$\gamma_0^2 \approx g_0^2 - i2g_0\bar{k} - \bar{k}^2 - 2\bar{k}k_1 \quad (2.6)$$

by neglecting the terms of order $g_0 k_1$ and k_1^2 . Since $k_1(z)$ is periodic we may expand it into the following complex Fourier series:

$$k_1(z) = \sum_{q=-\infty}^{\infty} b_q \exp(i2qK_B z), \quad (2.6)$$

where the coefficients b_q are complex in general.

Equation (2.1) then becomes

$$\frac{d^2 E}{dz^2} - (g_0 - i\bar{k})^2 E = [-2\bar{k} \sum_{q=-\infty}^{\infty} b_q \exp(i2qK_B z)] E. \quad (2.7)$$

Since the general solution of Equation (2.1) or (2.7) is given by the Floquet form (2.4), and $\phi(z)$, $\psi(z)$ are periodic, $E(z)$ may also be expanded into the following form:

$$\begin{aligned}
E(z) &= \sum_{q=-\infty}^{\infty} u_q^f \exp(\Gamma_0 z + i2qK_B z) \\
&+ \sum_{q=-\infty}^{\infty} u_q^b \exp(-\Gamma_0 z + i2qK_B z). \quad (2.8)
\end{aligned}$$

Calculating $\frac{d^2 E}{dz^2}$ we find

$$\begin{aligned}
\frac{d^2 E}{dz^2} &= \sum_{q=-\infty}^{\infty} (\Gamma_0 + i2qK_B)^2 u_q^f \exp(\Gamma_0 z + i2qK_B z) \\
&+ \sum_{q=-\infty}^{\infty} (-\Gamma_0 + i2qK_B)^2 u_q^b \exp(-\Gamma_0 z + i2qK_B z). \quad (2.9)
\end{aligned}$$

Substituting Equations (2.8) and (2.9) into Equation (2.7) yields

$$\begin{aligned}
&\sum_{q=-\infty}^{\infty} \{(\Gamma_0 + i2qK_B)^2 - (q_0 - i\bar{k})^2\} u_q^f \exp(\Gamma_0 z + i2qK_B z) \\
&+ \sum_{q=-\infty}^{\infty} \{(-\Gamma_0 + i2qK_B)^2 - (q_0 - i\bar{k})^2\} u_q^b \exp(-\Gamma_0 z + i2qK_B z) \\
&= -2\bar{k} \left\{ \sum_{p=-\infty}^{\infty} b_p \exp(i2pK_B z) \right\} \left[\sum_{q=-\infty}^{\infty} u_q^f \exp(\Gamma_0 z + i2qK_B z) \right. \\
&\quad \left. + \sum_{q=-\infty}^{\infty} u_q^b \exp(-\Gamma_0 z + i2qK_B z) \right]. \quad (2.10)
\end{aligned}$$

By collecting the coefficients of terms with similar exponents from Equation (2.10) and recalling that $b_0 = 0$, we

obtain a sequence of equations defining the coupling between the various orders of $E(z)$.

First, from the terms with $\exp(+\Gamma_0 z)$ we have

$$[\Gamma_0^2 - (g_0 - i\bar{k})^2] u_0^f = -2\bar{k} [b_{-1} u_1^f + b_{1-1} u_{-1}^f + \sum_{q=2}^{\infty} b_{-q} u_{+q}^f] \quad (2.11a)$$

$$[\Gamma_0^2 - (g_0 - i\bar{k})^2] u_0^b = -2\bar{k} [b_{-1} u_1^b + b_{1-1} u_{-1}^b + \sum_{q=-2}^{-\infty} b_{-q} u_{+q}^b] \quad (2.11b)$$

From the terms with $\exp(\Gamma_0 z + i2K_B z)$, we have

$$[(\Gamma_0 + i2K_B)^2 - (g_0 - i\bar{k})^2] u_1^f = -2\bar{k} [b_1 u_0^f + \sum_{q=2}^{\infty} \{b_q u_{1-q}^f + b_{1-q} u_q^f\}] \quad (2.12a)$$

$$[(\Gamma_0 - i2K_B)^2 - (g_0 - i\bar{k})^2] u_1^f = -2\bar{k} [b_{-1} u_0^f + \sum_{q=-2}^{-\infty} \{b_q u_{1+q}^f + b_{1+q} u_q^f\}] \quad (2.12b)$$

For the terms with $\exp(-\Gamma_0 z + i2K_B z)$ we have

$$[(-\Gamma_0 - i2K_B)^2 - (g_0 - i\bar{k})^2] u_1^b = -2\bar{k} [b_{-1} u_0^b + \sum_{q=-2}^{-\infty} \{b_q u_{1+q}^b + b_{1+q} u_q^b\}] \quad (2.13a)$$

$$\begin{aligned}
& [(-\Gamma_0 + i2K_B)^2 - (g_0 - i\bar{k})^2] u_1^b = -2\bar{k} [b_1 u_0^b \\
& + \sum_{q=2}^{\infty} \{b_q u_{1-q}^b + b_{1-q} u_q^b\}] \quad (2.13b)
\end{aligned}$$

In principle, this sequence could be extended indefinitely and the resulting system of equations solved for a dispersion equation relating Γ_0 to $(g_0 - i\bar{k}_0)$. However, since operation of a distributed feedback system is at or near the Bragg condition, we note that only first order harmonics should have significant amplitude and interaction. Hence, we truncate the series in Equations (2.11), (2.12) and (2.13) for $|q| \geq 2$. Furthermore, for a symmetric structure a proper choice of the origin gives $b_1 = -\underline{b}_1 = b^*$, where the asterisk denotes the complex conjugation. These restrictions of symmetry and choice of origin greatly simplify the following analysis although they are not essential physical restrictions. Elachi (71) and Peng (72) give a completely general method of developing the dispersion relation. Okuda and Kubo (73) gives results for asymmetrical structures.

Equations (2.11), (2.12) and (2.13) may now become respectively

$$[\Gamma_0^2 - (g_0 - i\bar{k})^2] u_f = 2\bar{k} b_1 [s^+ - s^-] u_f \quad (2.14a)$$

$$[\Gamma_0^2 - (g_0 - i\bar{k})^2] u_b = 2\bar{k} b_1 [s^+ - s^-] u_b \quad (2.14b)$$

$$u_1^f = s^+ u_f \quad (2.15a)$$

$$u_{-1}^f = s^- u_f \quad (2.15b)$$

$$u_{-1}^b = -s^+ u_b \quad (2.16a)$$

$$u_1^b = -s^- u_b \quad (2.16b)$$

where

$$u_0^f = u_f \quad (2.17a)$$

and

$$u_0^b = u_b \quad (2.17b)$$

$$s^+ = -2\bar{k}b_1 [(\Gamma_0 + i2K_B)^2 - (g_0 - i\bar{k})^2]^{-1} \quad (2.18a)$$

$$s^- = 2\bar{k}b_1 [(\Gamma_0 - i2K_B)^2 - (g_0 - i\bar{k})^2]^{-1} \quad (2.18b)$$

Recalling once more that the device operates near the Bragg condition, we now define

$$\delta = K_B - \bar{k} \quad (2.19a)$$

$$\delta_e = K_B - K_0 \quad (2.19b)$$

Recalling $\Gamma_0 = G_0 - iK_0$ and using Equations (2.19), Equation (2.18a) becomes

$$s^+ = -2(K_B - \delta)b_1 \{ [G_0 - i(K_B - \delta_e) + i2K_B]^2 - [g_0 - i(K_B - \delta)]^2 \}^{-1}. \quad (2.20)$$

It is easily shown that under the assumption:

$$|(G_0 + g_0) + i(\delta_e + \delta)| \ll 2K_B \quad (2.21)$$

Equation (2.20) is reduced to the following:

$$s^+ = \kappa [G_0 + g_0 + i(\delta_e + \delta)]^{-1}, \quad (2.22)$$

where $\kappa = ib_1$. (2.23)

It should be noted that b_1 is complex. For example, in the case $k_0(z)$ is given by Figure (3) b_1 is purely imaginary so that κ is real quantity.

Similarly Equation (2.18b) for s^- becomes

$$s^- = 2(K_B - \delta)b_1 \{ [G_0 - i(K_B - \delta_e) - i2K_B]^2 - [g_0 - i(K_B - \delta)]^2 \}^{-1}. \quad (2.24)$$

Again, with the assumption (2.21) as made in Equation (2.22),

$$s^- = i\kappa / (8K_B), \quad (2.25)$$

which is certainly negligible compared to s^+ .

Similar approximations may be used to justify neglect of the higher order modes of $E(z)$. In fact we may show that

(3)

$$|u_{\pm q}| \leq |\kappa [2q(1-q)K_B]^{-1}| u_0 \quad \text{for } |q| \geq 2. \quad (2.26)$$

Using the results from Equation (2.22) and neglecting s^- Equation (2.14) now becomes

$$\Gamma_0^2 - (g_0 - i\bar{\kappa})^2 = 2\bar{\kappa}b_1\kappa [G_0 + g_0 + i(\delta_e + \delta)]^{-1}. \quad (2.27)$$

As before, using Equations (2.19), Equation (2.27) becomes

$$[G_0 - i(K_B - \delta_e)]^2 - [g_0 - i(K_B - \delta)]^2 = 2\bar{\kappa}b_1\kappa[G_0 + g_0 + i(\delta_e + \delta)]^{-1}. \quad (2.28)$$

Using the condition (2.21), Equation (2.28) becomes

$$[g_0 + G_0 + i(\delta + \delta_e)][g_0 - G_0 + i(\delta - \delta_e)] = -\kappa^2 \quad (2.29)$$

or

$$[g_0^2 - G_0^2 + \delta_e^2 - \delta^2 + i2(g_0\delta - \delta_e G_0)] = -\kappa^2. \quad (2.30)$$

Since $-\kappa^2$ is real, then equating real and imaginary parts of (2.29) gives

$$G_0^2 - \delta_e^2 = \kappa^2 + g_0^2 - \delta^2 \quad (2.31)$$

$$G_0\delta_e = g_0\delta. \quad (2.32)$$

Summarizing our results we have a solution for the electric field given by

$$E(z) = u_f\phi(z) \exp(\Gamma_0 z) + u_b\psi(z) \exp(-\Gamma_0 z), \quad (2.33)$$

where

$$\Gamma_0 = G_0 - iK_0 \quad (2.34)$$

$$\phi(z) = 1 + s \exp(i2K_B z) \quad (2.35a)$$

$$\psi(z) = 1 - s \exp(-i2K_B z) \quad (2.35b)$$

$$s = \kappa[G_0 + g_0 + i(\delta_e + \delta)]^{-1} \quad (2.36)$$

$$\kappa = ib_1 \quad (2.23)$$

and

$$G_o^2 - \delta_e^2 = \kappa^2 + g_o^2 - \delta^2 \quad (2.31)$$

$$G_o \delta_e = g_o \delta . \quad (2.32)$$

The quantities $\delta = (K_B - \bar{k})$ and $\delta_e = (K_B - K_o)$ represent respectively the amount of detuning of \bar{k} and K_o away from the Bragg wave number K_B . Here \bar{k} is the phase constant of wave in a uniform nonperiodic medium, while K_o represents the phase constant in perfectly periodic medium. The quantity κ is the distributed feedback coefficient (coupling coefficient) defined as the average reflection per unit length. G_o and g_o are the effective gain constant of wave in a perfectly periodic medium and the gain constant of wave in the corresponding uniform nonperiodic medium respectively. G_o , δ_e , g_o and δ are related by Equation (2.31) and Equation (2.32). It is of interest to note that when $b_1 = 0$, i.e., the periodic variation of $k_o(z)$ is absent, $k(z) = \bar{k}$ and $\kappa = 0$. Equation (2.31) and Equation (2.32) suggest that $G_o = g_o$ and $\delta_e = \delta$ which is to be expected.

B. Propagation in a Perturbed Medium

Once we have the solution for $E(z)$ for a perfectly periodic medium, we may use this as a basis for a perturbation approximation which will account for small deviations from an ideal structure. These deviations are modelled by the addition of a zero mean random variable to the unperturbed propagation constant γ_0 .

Consider now the equation

$$\frac{d^2 E}{dz^2} - \gamma^2 E = 0, \quad (2.37)$$

where

$$\gamma = \gamma_0 + \gamma_r \quad (2.38a)$$

with

$$\overline{\gamma_r} = 0. \quad (2.38b)$$

Recall from the previous section that

$$E_0(z) = A\phi(z) \exp(\Gamma_0 z) + B\psi(z) \exp(-\Gamma_0 z) \quad (2.39)$$

is the general solution of

$$\frac{d^2 E}{dz^2} - \gamma_0^2 E_0 = 0 \quad (2.40)$$

with Γ_0 , ϕ , and ψ given by Equations (2.34), (2.35a) and (2.35b) respectively.

Assuming that the fundamental periodic nature remains essentially unaffected, we seek a solution of Equation

(2.37) of the form

$$E(z) = A\phi(z) \exp[\Gamma^+(z)] + B\psi(z) \exp[-\Gamma^-(z)]. \quad (2.41)$$

For convenience, define

$$\Phi(z) = \ln[\phi(z)] \quad (2.42a)$$

$$\Psi(z) = \ln[\psi(z)]. \quad (2.42b)$$

Then Equations (2.39) and (2.41) become, respectively:

$$E_0(z) = A \exp[\Phi(z) + \Gamma_0 z] + B \exp[\Psi(z) - \Gamma_0 z] \quad (2.43a)$$

and

$$E(z) = A \exp[\Phi(z) + \Gamma^+(z)] + B \exp[\Psi(z) - \Gamma^-(z)]. \quad (2.43b)$$

Calculating the derivatives of Equations (2.43) gives

$$\begin{aligned} \frac{d^2 E}{dz^2} = & A \left[\frac{d^2 \Phi}{dz^2} + \left(\frac{d\Phi}{dz} \right)^2 + 2\Gamma_0 \frac{d\Phi}{dz} + \Gamma_0^2 \right] \exp(\Phi + \Gamma_0 z) \\ & + B \left[\frac{d^2 \Psi}{dz^2} + \left(\frac{d\Psi}{dz} \right)^2 - 2\Gamma_0 \frac{d\Psi}{dz} + \Gamma_0^2 \right] \exp(\Psi - \Gamma_0 z) \end{aligned} \quad (2.44a)$$

$$\begin{aligned} \frac{d^2 E}{dz^2} = & A \left[\frac{d^2}{dz^2} (\Phi + \Gamma^+) + \left(\frac{d\Phi}{dz} \right)^2 + 2 \left(\frac{d\Gamma^+}{dz} \right) \left(\frac{d\Phi}{dz} \right) \right. \\ & \left. + \left(\frac{d\Gamma^+}{dz} \right)^2 \right] \exp(\Phi + \Gamma^+) + B \left[\frac{d^2}{dz^2} (\Psi - \Gamma^-) + \left(\frac{d\Psi}{dz} \right)^2 \right. \\ & \left. - 2 \left(\frac{d\Gamma^-}{dz} \right) \left(\frac{d\Psi}{dz} \right) + \left(\frac{d\Gamma^-}{dz} \right)^2 \right] \exp(\Psi - \Gamma^-). \end{aligned} \quad (2.44b)$$

Substituting Equations (2.43b) and (2.44b) into Equation (2.37) we obtain:

$$\begin{aligned}
 & A \left[\frac{d^2}{dz^2} (\Phi + \Gamma^+) + \left(\frac{d\Phi}{dz} \right)^2 + 2 \left(\frac{d\Gamma^+}{dz} \right) \left(\frac{d\Phi}{dz} \right) \right. \\
 & \quad \left. + \left(\frac{d\Gamma^+}{dz} \right)^2 - \gamma^2 \right] \exp(\Phi + \Gamma^+) \\
 & + B \left[\frac{d^2}{dz^2} (\Psi - \Gamma^-) + \left(\frac{d\Psi}{dz} \right)^2 - 2 \left(\frac{d\Gamma^-}{dz} \right) \left(\frac{d\Psi}{dz} \right) \right. \\
 & \quad \left. + \left(\frac{d\Gamma^-}{dz} \right)^2 - \gamma^2 \right] \exp(\Psi - \Gamma^-) = 0. \tag{2.45}
 \end{aligned}$$

Considering the exponentials as orthogonal functions the coefficients of the two terms in Equation (2.45) must be independently equal to zero.

$$\frac{d^2}{dz^2} (\Phi + \Gamma^+) + \left(\frac{d\Phi}{dz} \right)^2 + 2 \left(\frac{d\Gamma^+}{dz} \right) \left(\frac{d\Phi}{dz} \right) + \left(\frac{d\Gamma^+}{dz} \right)^2 - \gamma^2 = 0. \tag{2.46a}$$

$$\frac{d^2}{dz^2} (\Psi - \Gamma^-) + \left(\frac{d\Psi}{dz} \right)^2 - 2 \left(\frac{d\Gamma^-}{dz} \right) \left(\frac{d\Psi}{dz} \right) + \left(\frac{d\Gamma^-}{dz} \right)^2 - \gamma^2 = 0 \tag{2.46b}$$

Similarly, Equations (2.43a), (2.44a), and (2.40) yield

$$\frac{d^2\Phi}{dz^2} + \left(\frac{d\Phi}{dz} \right)^2 + 2\Gamma_0 \frac{d\Phi}{dz} + \Gamma_0^2 - \gamma_0^2 = 0 \tag{2.47a}$$

$$\frac{d^2\Psi}{dz^2} + \left(\frac{d\Psi}{dz} \right)^2 - 2\Gamma_0 \frac{d\Psi}{dz} + \Gamma_0^2 - \gamma_0^2 = 0. \tag{2.47b}$$

Subtracting (2.47) from (2.46) we obtain

$$\frac{d^2 \Gamma^+}{dz^2} + 2 \frac{d\phi}{dz} \left(\frac{d\Gamma^+}{dz} - \Gamma_0 \right) + \left(\frac{d\Gamma^+}{dz} \right)^2 - \Gamma_0^2 - \Delta\gamma = 0 \quad (2.48)$$

$$\frac{d^2 \Gamma^-}{dz^2} - 2 \frac{d\psi}{dz} \left(\frac{d\Gamma^-}{dz} - \Gamma_0 \right) + \left(\frac{d\Gamma^-}{dz} \right)^2 - \Gamma_0^2 - \Delta\gamma = 0, \quad (2.48b)$$

$$\text{where } \Delta\gamma = (\gamma^2 - \gamma_0^2) \quad (2.49)$$

Since for reasonable perturbations, we expect $\Gamma^+(z)$ to be fairly close to $\Gamma_0 z$ and $\frac{d\Gamma^+}{dz}$ to be fairly close to Γ_0 , we might also expect $\frac{d^2 \Gamma^+}{dz^2}$ to be nearly zero. Therefore, to effect an approximate solution for $\Gamma^+(z)$, we neglect $\frac{d^2 \Gamma^+}{dz^2}$ in Equation (2.48). Then

$$2 \left(\frac{d\phi}{dz} \right) \left(\frac{d\Gamma^+}{dz} - \Gamma_0 \right) + \left(\frac{d\Gamma^+}{dz} + \Gamma_0 \right) \left(\frac{d\Gamma^+}{dz} - \Gamma_0 \right) - \Delta\gamma = 0. \quad (2.50)$$

When solved for $\frac{d\Gamma^+}{dz}$, as $\Delta\gamma$ approaches zero, the roots of Equation (2.50) approach Γ_0 and $(-\Gamma_0 - 2\frac{d\phi}{dz})$. Certainly the choice for the solution should be such that it approaches to Γ_0 as $\Delta\gamma \rightarrow 0$.

Equation (2.50), being a quadratic in $\frac{d\Gamma^+}{dz}$, can be solved analytically as

$$\frac{d\Gamma^+}{dz} = \Gamma_0 + \frac{d\phi}{dz} + \left[\left(\frac{d\phi}{dz} + \Gamma_0 \right)^2 + \Delta\gamma \right]^{1/2}, \quad (2.51)$$

which can be approximated by

$$\frac{d\Gamma^+}{dz} \approx -\frac{d\phi}{dz} \pm \left[\left(\frac{d\phi}{dz} + \Gamma_0 \right) + \frac{\Delta\gamma}{2} \left(\frac{d\phi}{dz} + \Gamma_0 \right)^{-1} \right], \quad (2.52)$$

provided that

$$|\Delta\gamma| \ll \left| \left(\frac{d\phi}{dz} + \Gamma_0 \right) \right|^2. \quad (2.53a)$$

The upper sign in Equation (2.52) gives a solution consistent with the previous discussion:

$$\frac{d\Gamma^+}{dz} \approx \Gamma_0 + \left(\frac{\Delta\gamma}{2} \frac{d\phi}{dz} + \Gamma_0 \right)^{-1}. \quad (2.53b)$$

Similarly,

$$\frac{d\Gamma^-}{dz} \approx \Gamma_0 + \frac{\Delta\gamma}{2} \left(-\frac{d\psi}{dz} + \Gamma_0 \right)^{-1}. \quad (2.54)$$

The assumption inherent in deriving Equations (2.53) and (2.54) is

$$\left| \frac{\frac{d^2\Gamma^+}{dz^2}}{\left(\frac{d\Gamma^+}{dz} \right)^2 - \Gamma_0^2} \right| \ll 1, \quad (2.55)$$

To verify the legitimacy of Equation (2.55) consider the following key terms. First:

$$\frac{d^2\Gamma^+}{dz^2} = \frac{d}{dz} \left[\Gamma_0 + \frac{\Delta\gamma}{2} \left(\frac{d\phi}{dz} + \Gamma_0 \right)^{-1} \right] \quad (2.56)$$

$$= \frac{d}{dz} \left(\frac{\Delta\gamma}{2} \right) \left[\frac{d\phi}{dz} + \Gamma_0 \right]^{-1} - \frac{\Delta\gamma}{2} \left(\frac{d^2\phi}{dz^2} \right) \left[\frac{d\phi}{dz} + \Gamma_0 \right]^{-2}. \quad (2.57)$$

Recall

$$\frac{d\phi}{dz} = \frac{d}{dz} \ln \phi = \frac{1}{\phi} \frac{d\phi}{dz}. \quad (2.58)$$

Extracting from Equation (2.35), we have

$$\frac{d\phi}{dz} = i2K_B s \exp(i2K_B z) [1 + s \exp(i2K_B z)]^{-1}, \quad (2.59)$$

and

$$\frac{d^2\phi}{dz^2} = \frac{-4K_B^2 s \exp(i2K_B z)}{1+s \exp(i2K_B z)} + \frac{4K_B^2 s^2 \exp(i2K_B z)}{[1+s \exp(i2K_B z)]^2}. \quad (2.60)$$

If $|s| \ll 1$, then

$$\frac{d\phi}{dz} \approx i2K_B s \exp(i2K_B z), \quad (2.61)$$

and

$$\frac{d^2\phi}{dz^2} \approx -4K_B^2 s \exp(i2K_B z). \quad (2.62)$$

Using results from Equations (2.61), (2.19)

$$\left[\frac{d\phi}{dz} + \Gamma_0\right] \approx i2K_B s \exp(i2K_B z) + G_0 - i(K_B - \delta_e), \quad (2.63)$$

which can be approximated by

$$\left[\frac{d\phi}{dz} + \Gamma_0\right] \approx -iK_B. \quad (2.64)$$

Turning now to

$$\left(\frac{d\Gamma^+}{dz}\right)^2 - \Gamma_0^2 = \Gamma_0 \Delta\gamma \left[\frac{d\phi}{dz} + \Gamma_0\right]^{-1} + \left(\frac{\Delta\gamma}{2}\right)^2 \left[\frac{d\phi}{dz} + \Gamma_0\right]^{-2}, \quad (2.65)$$

which can be reduced to the following; with the aid of Equation (2.53) and (2.64)

$$\left(\frac{d\Gamma^+}{dz}\right)^2 - \Gamma_0^2 \approx \Delta\gamma. \quad (2.66)$$

Finally by combining Equation (2.57) and (2.66), Equation (2.55) becomes

$$\left| \frac{\frac{d^2 \Gamma^+}{dz^2}}{\left(\frac{d\Gamma^+}{dz}\right)^2 - \Gamma_0^2} \right| \approx \frac{1}{2K_B} \left| \frac{\frac{d}{dz}(\Delta\gamma)}{\Delta\gamma} \right| + 2s \ll 1. \quad (2.67)$$

Certainly the $2s$ term is negligible.

To pinpoint the first term of the right side of Equation (2.67): examine first:

$$\frac{1}{2K_B} \left| \frac{\frac{d}{dz} \Delta\gamma}{\Delta\gamma} \right| = \frac{1}{2K_B} \left| \frac{\frac{d}{dz}(2\gamma_0\gamma_r + \gamma_r^2)}{(2\gamma_0\gamma_r + \gamma_r^2)} \right| \quad (2.68)$$

Since

$$2\gamma_0\gamma_r \gg \gamma_r^2,$$

$$\frac{1}{2K_B} \frac{1}{\Delta\gamma} \frac{d\Delta\gamma}{dz} \approx \frac{1}{2K_B} \left[\frac{1}{\gamma_0} \frac{d\gamma_0}{dz} + \frac{1}{\gamma_r} \frac{d\gamma_r}{dz} + \frac{1}{\gamma_0} \frac{d\gamma_r}{dz} \right]. \quad (2.69)$$

For γ_0 as earlier specified, the first and third terms will be negligible. The term $\frac{1}{2K_B} \left| \frac{1}{\gamma_r} \frac{d\gamma_r}{dz} \right|$ will be significantly less than unity if the spatial spectral bandwidth of γ_r is well below $2K_B$. Alternatively, γ_r must vary slowly when compared to a wavelength.

Equations (2.53) and (2.54) may then be integrated to give $\Gamma^+(z)$ and $\Gamma^-(z)$ as required.

C. Threshold Condition for Perturbed Media

Using the results from the two previous sections we now derive an expression relating the threshold gain and resonance frequency for a distributed feedback laser with a structure not perfectly periodic.

Consider the pure distributed feedback case with no end reflections other than those induced by the periodic nature of the medium. Suppose we have a periodic structure extending from $z = -L/2$ to $z = +L/2$ with the origin chosen so as to satisfy the symmetry requirements of Section A, as shown in Figure 5. The propagation within the periodic region is given by

$$E_p^f = u_f \exp[\phi(z) + \Gamma^+(z)] \quad (2.70a)$$

$$E_p^b = u_b \exp[\psi(z) - \Gamma^-(z)], \quad (2.70b)$$

where

$$\frac{d\Gamma^+}{dz} = \Gamma_0 + \frac{\Delta\gamma}{2} [\Gamma_0 + \frac{d\phi}{dz}]^{-1} \quad (2.71a)$$

$$\frac{d\Gamma^-}{dz} = \Gamma_0 + \frac{\Delta\gamma}{2} [\Gamma_0 - \frac{d\psi}{dz}]^{-1}. \quad (2.71b)$$

The propagation outside the periodic region is given by

$$E^{f,b}(z) = E_{f,b} \exp(\mp i\beta z). \quad (2.72)$$

For the structure as shown in Figure 5, interior reflection coefficients can be defined at $z = \pm L/2$.

Assuming the medium has homogeneous linear magnetic properties and using the continuity of tangential electric and magnetic fields, at $z = \pm L/2$, the reflection coefficients at the interior boundaries are given (3) by

$$R_1 = (Y_B - Y_O) / (Y_F + Y_O) \quad (2.73a)$$

$$R_2 = (Y_F - Y_O) / (Y_B + Y_O), \quad (2.73b)$$

where

$$Y_F = \frac{d\Gamma^+}{dz} + \frac{d\phi}{dz} = \Gamma_O + \frac{d\phi}{dz} + \epsilon_f \quad (2.74a)$$

$$Y_B = \frac{d\Gamma^-}{dz} - \frac{d\psi}{dz} = \Gamma_O - \frac{d\psi}{dz} + \epsilon_b \quad (2.74b)$$

$$Y_O = -i\beta \quad (2.74c)$$

$$\epsilon_f = \frac{\Delta\gamma}{2} [\Gamma_O + \frac{d\phi}{dz}]^{-1} \quad (2.74d)$$

$$\epsilon_b = \frac{\Delta\gamma}{2} [\Gamma_O - \frac{d\psi}{dz}]^{-1}. \quad (2.74e)$$

The condition for lasing is that the net propagation along a path from $z = -L/2$ to $z = +L/2$ to $z = -L/2$ is lossless and in phase, i.e.,

$$R_1 R_2 \exp(\xi + \eta) = 1, \quad (2.75)$$

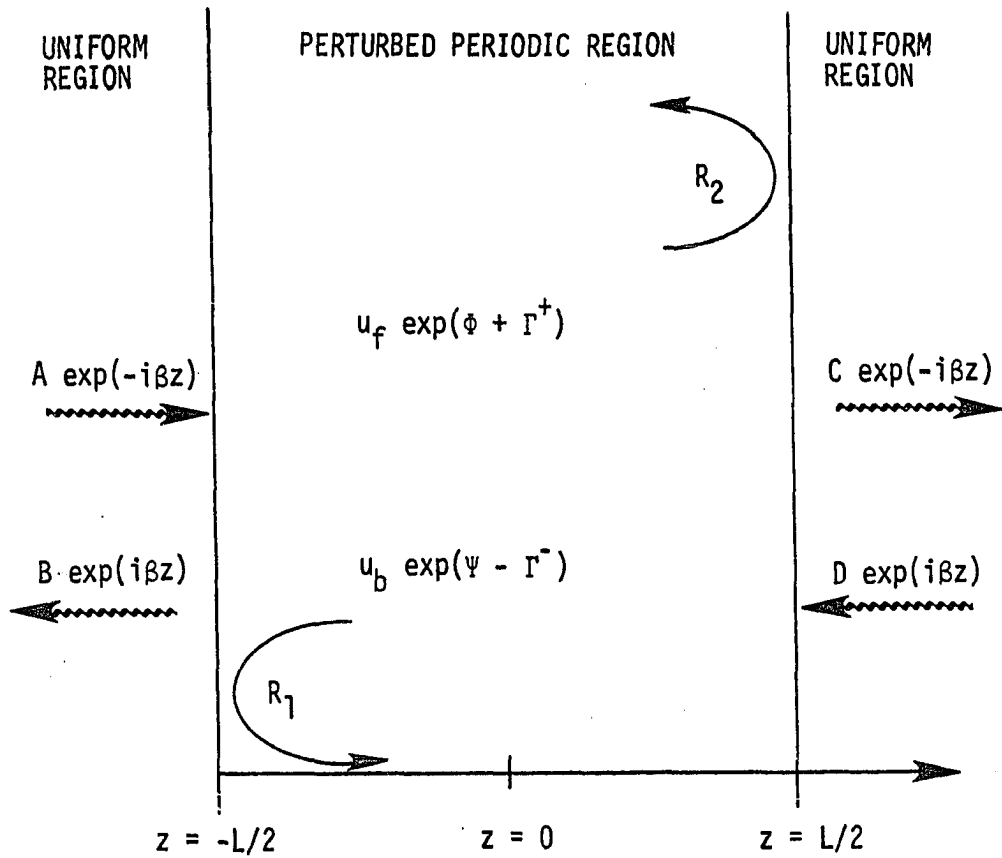


Figure 5. Diagram showing reflection and transmission at the boundaries between uniform and perturbed periodic regions

where

$$\xi = \phi(L/2) - \phi(-L/2) + \psi(-L/2) - \psi(L/2) \quad (2.76a)$$

$$\eta = \Gamma^+(L/2) - \Gamma^+(-L/2) + \Gamma^-(L/2) - \Gamma^-(-L/2) \quad (2.76b)$$

or

$$\eta = \int_{-\frac{L}{2}}^{\frac{L}{2}} \frac{d\Gamma^+}{dz} dz + \int_{-\frac{L}{2}}^{\frac{L}{2}} \frac{d\Gamma^-}{dz} dz . \quad (2.76c)$$

Recalling Equations (2.53) and (2.54) for $\frac{d\Gamma^+}{dz}$ Equation (2.76c) becomes

$$\eta = \eta_o + \eta_r , \quad (2.77)$$

where

$$\eta_o = 2L\Gamma_o \quad (2.78)$$

$$\eta_r = \int_{-\frac{L}{2}}^{\frac{L}{2}} (\epsilon_b + \epsilon_f) dz . \quad (2.79)$$

Recall the approximate solutions for ϕ, ψ from Equation (2.35)

$$\phi = 1+s \exp(i2K_B z) \quad (2.35)$$

$$\psi = 1-s \exp(-i2K_B z) .$$

Examining first the term $\exp(\xi)$, defined as

$$\exp(\xi) = \frac{\phi(\frac{L}{2})\psi(-\frac{L}{2})}{\phi(-\frac{L}{2})\psi(\frac{L}{2})} \quad (2.80-2.81)$$

with the aid of Equation (2.35) we have

$$\exp(\xi) = \frac{[1+s \exp(iLK_B)][1-s \exp(iLK_B)]}{[1+s \exp(-iLK_B)][1-s \exp(-iLK_B)]} \quad (2.82)$$

or

$$\exp(\xi) = \frac{1-s^2 \exp(i2K_B L)}{1-s^2 \exp(-i2K_B L)} \quad (2.83)$$

Assuming that $s \ll 1$, Equation (2.83) gives

$$\exp(\xi) \approx 1. \quad (2.84)$$

The reflection coefficient is given by

$$R_1 = \frac{\Gamma_0 - i2K_B s \exp(-i2K_B z) [1-s \exp(-i2K_B z)]^{-1+\epsilon_b+i\beta}}{\Gamma_0 + i2K_B s \exp(i2K_B z) [1+s \exp(i2K_B z)]^{-1+\epsilon_f-i\beta}} \Big|_{z = -\frac{L}{2}} \quad (2.85)$$

With the aid of Equation (2.19), and neglecting terms of order G , δ , ϵ relative to K_B and orders s relative to unity, R_1 may be approximated by

$$R_1 \approx s \exp(-i2K_B z) \Big|_{z = -\frac{L}{2}} = s \exp(iK_B L). \quad (2.86)$$

Note that ϵ_f and ϵ_b , the terms determined by the perturbation, have virtually no effect on R_1 .

Similarly:

$$R_2 \approx -s \exp(i2K_B z) \Big|_{z = \frac{L}{2}} = -s \exp(iK_B L) \quad (2.87)$$

The threshold Equation (2.75) then becomes

$$-s^2 \exp[i2K_B L + 2\Gamma_O L + \eta_r] = 1 \quad (2.88)$$

or

$$-s^2 \exp(\eta_r) \exp[2(G_O + i\delta_e)L] = 1. \quad (2.89)$$

The absolute magnitude of Equation (2.89) determines the threshold gain needed for laser action, whereas the phase of Equation (2.89) determines the longitudinal mode of laser oscillation.

By using the expression of the coupling constant, s , given by Equation (2.36), Equation (2.88) becomes

$$-\kappa^2 [G_O + g_O + i(\delta_e + \delta)]^{-2} \exp[\eta_r + 2L(G_O + i\delta_e)] = 1. \quad (2.90)$$

By taking the square root of Equation (2.90) we obtain

$$\begin{aligned} \kappa \exp(\eta_r/2) \exp[(G_O + i\delta_e)L] \\ = \pm i [G_O + g_O + i(\delta_e + \delta)]. \end{aligned} \quad (2.91)$$

Using the fact that

$$\exp(\theta) = [\sinh \theta + \cosh \theta] \quad (2.92)$$

Equation (2.91) can be rearranged to give

$$\kappa \exp\left(\frac{\eta_r}{2}\right) \sinh[(G_O + i\delta_e)L] = \pm i (G_O + i\delta_e) \quad (2.93a)$$

and

$$\kappa \exp\left(\frac{\eta_r}{2}\right) \cosh[(G_O + i\delta_e)L] = \pm i (g_O + i\delta). \quad (2.93b)$$

For convenience of discussion, if we define the following dimensionless parameters of interest:

$$x = (G_0 L), \quad y = (\delta_e L), \quad x_0 = (g_0 L)$$

$$y_0 = (\delta L), \quad \tilde{p} = \frac{\eta_r}{2} \quad \text{and} \quad \tau = (\kappa L) \quad (2.94)$$

then Equation (2.91) and (2.93) can be expressed respectively:

$$\tau \exp(p) \exp[x+iy] = \underline{\pm} i [(x+x_0)+i(y+y_0)] \quad (2.95)$$

$$\tau \exp(p) \sinh(x+iy) = \underline{\pm} i (x+iy) \quad (2.96a)$$

$$\tau \exp(p) \cosh(x+iy) = \underline{\pm} i (x_0+iy_0). \quad (2.96b)$$

It should be noted that the perturbation parameter $p = \eta_r/2$ where η_r is as defined by Equation (2.79), represents the effect of the irregularity in the periodic medium, either due to the inhomogeneity in thin-film material, or due to the irregularity in the periodicity in the periodic structure. η_r is a complex quantity in general. As $\eta_r \rightarrow 0$, $p \rightarrow 0$ and Equation (2.96a) and Equation (2.96b) become

$$\tau \sinh(x+iy) = \underline{\pm} i (x+iy) \quad (2.97a)$$

$$\tau \cosh(x+iy) = \underline{\pm} i (x_0+iy_0) \quad (2.97b)$$

which is the threshold condition for the perfectly periodic case. This is the form, first given by Kogelnik and Shank (2), and considered by Wang (3) for the analysis of a DFB

laser with a perfectly periodic structure.

By separating the real and the imaginary part of Equation (2.97a) we obtain

$$\tau \cosh x \sin y = x \quad (2.98a)$$

$$\tau \sinh x \cos y = -y \quad (2.98b)$$

and similarly from Equation (2.97b), we have

$$\tau \sinh x \sin y = x_0 \quad (2.99a)$$

$$\tau \cosh x \cos y = -y_0. \quad (2.99b)$$

By combining Equation (2.98a) and Equation (2.99a),

$$\tau e^x \sin y = (x+x_0) \quad (2.100a)$$

and from Equation (2.98b) and Equation (2.99b)

$$\tau e^x \cos y = -(y+y_0). \quad (2.100b)$$

On the other hand, from Equation (2.31) and Equation (2.32) with the aid of Equation (2.94) we have

$$x^2 - y^2 = \tau^2 + x_0^2 - y_0^2 \quad (2.101a)$$

and

$$xy = x_0 y_0. \quad (2.101b)$$

Thus we have a system of four equations which relate five parameters; x , y , x_0 , y_0 and τ . These equations can be rearranged into the following forms:

$$x_0 = -y \tan y \quad (2.102a)$$

$$x \tanh x = x_0 \quad (2.102b)$$

$$y_0 = xy/x_0 \quad (2.102c)$$

$$\tau = e^{-x} \sqrt{(x+x_0)^2 + (y+y_0)^2} \quad (2.102d)$$

The variation of the gain parameters $x = (G_0 L)$, $x_0 = (g_0 L)$ and the phase parameters $y = (\delta_e L)$ and $y_0 = (\delta L)$ with the coupling parameter $\tau = (\kappa L)$ can be studied with the aid of Equations (2.102a-2.102d). The plots of x , y , x_0 and y_0 versus τ are shown in Figure 6. It should be pointed out that the plot of x_0 vs. τ has previously been plotted by Kogelnik and Shank (2), and also by Wang (3). We shall use these plots in the Section III for the investigation of the effect of the presence of perturbation parameter p . In the meantime, it is interesting to observe, from Figure 6, that as $\tau \rightarrow 0$ (i.e., $\kappa_1 \rightarrow 0$), $x \rightarrow x_0$ and $y \rightarrow y_0$, i.e., $G_0 \rightarrow g_0$ and $\delta_e \rightarrow \delta$ or $K_0 \rightarrow \bar{k}$. On the other hand, in the range of large τ , the values of x and x_0 can be significantly different while the values of y and y_0 can be quite different from each other.

To facilitate our discussion, we can divide DFB laser operation into three categories, according to the behavior of the gain parameter x_0 ; "weakly coupled case" (case A),

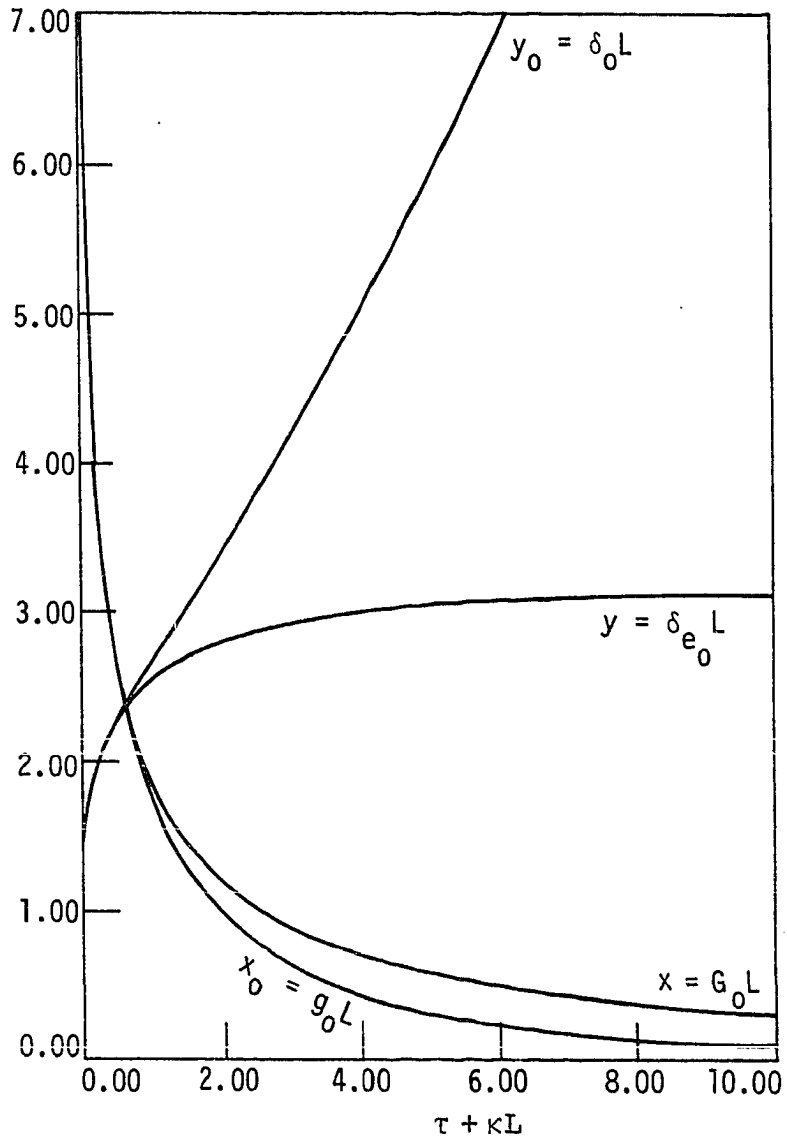


Figure 6. The variation of the gain parameters x , x_0 and phase parameters y, y_0 with the coupling parameter τ for a perfectly periodic structure. $x = (G_0 L)$, $x_0 = (g_0 L)$, $y = (\delta_e L)$, $y_0 = (\delta_0 L)$, $\tau = (\kappa L)$

where $\tau^2 \ll x_0^2$ (or $\kappa^2 \ll g_0^2$), "moderately coupled case" (case B) where τ and x_0 are same order of magnitude, and "strongly coupled case" (case C) where $\kappa^2 \gg g_0^2$.

For case A, $x=x_0$, and $y=y_0$ so that the effective propagation constant $\Gamma_0 = (G_0 - iK_0)$ is approximately the same as $\gamma_0 = (g_0 - i\bar{k})$ for the corresponding uniform waveguide. However, for case C, Γ_0 can be quite different from γ_0 . The asymptotic behavior of the parameters, x , y , x_0 and y_0 can be investigated using Equations (2.102a-2.102d). As $\tau \rightarrow 0$ (i.e., $\kappa \rightarrow 0$), in other words, as the coupling strength approaches zero, $x \rightarrow \infty$, from Equation (2.102d). We observe from Equation 102b that as $x \rightarrow \infty$, $\tanh x \rightarrow 1$ so that $x \rightarrow x_0$ and consequently $y \rightarrow y_0$ which is apparent from Equation (2.102c). In order to satisfy Equation (2.102a), the value of y must be in the range, $(2n-1)\frac{\pi}{2} < y < (2n+1)\frac{\pi}{2}$, where n is a positive integer. As $x \rightarrow x_0 \rightarrow \infty$ and $y \rightarrow y_0$, which must approach $(2n-1)\frac{\pi}{2}$. For example, for $n=1$, $(\delta L) \rightarrow \frac{\pi}{2}$. On the other hand, as $x_0 = (g_0 L) \rightarrow 0$, from Equation (2.102a) we observe $(\delta_e L) = y \rightarrow \pi$, while from Equation (2.102b) $x^2 \approx x_0 \rightarrow 0$ so that $y_0 = y/\sqrt{x_0}$, from Equation (2.102c). As $x_0 \rightarrow 0$, $y \rightarrow \pi$, $y_0 \rightarrow \infty$ and from Equation (2.102d) $\tau \rightarrow y_0 \rightarrow \infty$, which is also apparent from Figure 6. Thus, for a weakly coupled case in which for sufficiently small τ and large x_0 , we have the following asymptotic expression, obtained from Equation (2.102d) and Equation (2.102a) respectively,

$$\tau \approx 2x_0 e^{-x_0} \quad (2.103)$$

and

$$y_0 \approx \pi/2 \quad (\text{case A})$$

On the other hand, for a strongly coupled case in which τ is sufficiently large and x_0 is small, we have the following:

$$\tau \approx \pi + y_0 \quad (2.104)$$

and

$$y \approx \pi \quad (\text{Case C}).$$

III. EFFECT OF PERTURBATION OF PERIODIC MEDIUM ON THE THRESHOLD CONDITION

In this section we shall study the effect of the presence of a perturbation in the periodic medium (or structure) in a DFB laser. To estimate this effect, from the perturbed threshold condition (2.93), we obtain the approximated expressions for the change in the gain parameter and in the phase parameter as a linear function of the perturbation parameter with the aid of truncated complex Maclaurin series expansion. To see how significant is the effect under consideration we shall obtain the plots showing the variation of the gain parameters and the phase parameters with the coupling parameter for different values of a properly specified perturbation parameter. The specification of the perturbation parameter depends on a particular statistical model used, and for the present study, we shall use the statistics of a first order stationary Gauss-Markov process.

A. Approximate Expression for the Perturbed Gain Parameters and Phase Parameters

The perturbed threshold condition, given by Equation (2.93a) and Equation (2.93b) can be expressed in the following form, with the aid of Equation (2.94):

$$-i\tau \exp(\tilde{p}) \sinh(\tilde{w}) = \tilde{w} \quad (3.1a)$$

and

$$-i\tau \exp(\tilde{p}) \cosh(\tilde{W}) = \tilde{w}, \quad (3.1b)$$

where

$$\tilde{W} = (\bar{x} + i\bar{y}) \quad \tilde{w} = (\bar{x}_0 + i\bar{y}_0)$$

and

$$\tilde{p} = (p_1 + ip_2). \quad (3.1c)$$

Here the symbol bar is placed on the quantity to emphasize the fact that the perturbed case is being considered, while the symbol tilde is placed on the letter to emphasize that a complex quantity is being considered.

It should be noted that as $\tau \rightarrow 0$, $\bar{x} \rightarrow x$, $\bar{y} \rightarrow y$, $\bar{x}_0 \rightarrow x_0$ and $\bar{y}_0 \rightarrow y_0$ in which the parameters x , y , x_0 and y_0 are as defined in Equation (2.94).

The functions $\tilde{W}(\tilde{p})$ and $\tilde{w}(\tilde{p})$, being analytic, can be expressed in terms of a complex Taylor series, or Maclaurin series expansion in the perturbation parameter \tilde{p} and the point $\tilde{p}=0$, since our point of reference is the unperturbed configuration. If the perturbation is small so that only the lower-order term in the series expansion contribute significantly, then we have the following approximate expressions for the effective propagation parameter $\tilde{W}(\tilde{p})$ in the periodic medium and the propagation parameter $\tilde{w}(\tilde{p})$ in the corresponding nonperiodic medium;

$$\tilde{w}(\tilde{p}) = \tilde{w}_0 + \left. \frac{d\tilde{w}}{d\tilde{p}} \right|_{\tilde{p}=0} \tilde{p} \quad (3.2a)$$

$$\tilde{w}(\tilde{p}) = \tilde{w}_0 + \left. \frac{d\tilde{w}}{d\tilde{p}} \right|_{\tilde{p}=0} \tilde{p}, \quad (3.2b)$$

where

$$\tilde{w}_0 = (x+iy) \text{ and } \tilde{w}_0 = (x_0+iy_0), \quad (3.2c)$$

in which x , y , x_0 , and y_0 are as defined in Equation (2.94) and satisfy the relations given by Equations (2.102a-2.102d).

The coefficient of the second term of the right-hand side of Equation (3.2a) and Equation (3.2b) can be easily evaluated to give

$$\left. \frac{d\tilde{w}}{d\tilde{p}} \right|_{\tilde{p}=0} = \left. \frac{\tilde{w}}{1-\tilde{w}} \right|_{\tilde{p}=0} = \frac{\tilde{w}_0}{(1-\tilde{w}_0)} \quad (3.3a)$$

and

$$\left. \frac{d\tilde{w}}{d\tilde{p}} \right|_{\tilde{p}=0} = \left. \left\{ \tilde{w} + \frac{\tilde{w}^2}{1-\tilde{w}} \right\} \right|_{\tilde{p}=0} = \frac{\tilde{w}_0 - \tilde{w}_0^2 + \tilde{w}_0^2}{(1-\tilde{w}_0)}. \quad (3.3b)$$

It should be pointed out that two types of perturbation may be present; type (A), in which the perturbation is mainly due to the irregularity in a physical parameter of the material from which the periodic structure is constructed, and type (B), in which the perturbation is mainly due to a geometrical factor, for example, the irregularity in the spatial periodicity of the structure.

Upon substitution of Equation (3.2c) into Equation (3.3b) we have

$$\left. \frac{d\tilde{w}}{d\tilde{p}} \right|_{\tilde{p}=0} = A_1 + iA_2, \quad (3.4a)$$

where

$$A_1 = \frac{(1-x_0)(x_0 + \tau^2) - y_0^2}{(1-x_0)^2 + y_0^2} \quad (3.5a)$$

$$A_2 = \frac{y_0(1 + \tau^2)}{(1-x_0)^2 + y_0^2}, \quad (3.5b)$$

and similarly, substitution of Equation (3.2c) into Equation (3.3a) gives

$$\left. \frac{d\tilde{w}}{d\tilde{p}} \right|_{\tilde{p}=0} = B_1 + iB_2, \quad (3.6)$$

where

$$B_1 = \frac{x - (x_0 x + y_0 y)}{(1-x_0)^2 + y_0^2} \quad (3.7a)$$

$$B_2 = \frac{y - x_0 y + x y_0}{(1-x_0)^2 + y_0^2}. \quad (3.7b)$$

Since the perturbation parameter \tilde{p} is complex, in general, by letting $\tilde{p} = (p_1 + ip_2)$ in Equation (3.2b) then separating the real and the imaginary parts of Equation (3.2b), we obtain

$$\bar{x}_0 = x_0 + (A_1 p_1 - A_2 p_2) \quad (3.8)$$

and

$$\bar{y}_0 = y_0 + (A_2 p_1 + A_1 p_2). \quad (3.9)$$

Similarly, by substituting Equation (3.6) into Equation (3.2a), we obtain

$$\bar{x} = x + (B_1 p_1 - B_2 p_2) \quad (3.10)$$

$$\bar{y} = y + (B_2 p_1 + B_1 p_2). \quad (3.11)$$

Recall that the dimensionless parameters x , y , x_0 and y_0 are for the case of a perfectly periodic medium whose variation with the coupling parameter was previously shown in Figure 6. In order to study how \bar{x} and \bar{y} vary with the coupling parameter τ , we must specify the value of the perturbation parameter \tilde{p} .

Using the approximation made in Equation (2.64), the factors ϵ_f and ϵ_b as defined in Equation (2.74d) and Equation (2.74e) can be expressed as $\epsilon_f = \epsilon_b = \left(\frac{i\Delta\gamma}{2K_B}\right)$, so that from Equation (2.79) and Equation (2.94) we can write the perturbation parameter \tilde{p} as follows:

$$\tilde{p} = \frac{i}{2K_B} \int_{-\frac{L}{2}}^{\frac{L}{2}} (\Delta\gamma) dz, \quad (3.12)$$

$$\text{where } \Delta\gamma = (\gamma^2 - \gamma_0^2), \quad (3.13a)$$

in which $\gamma_0 = (g_0 - i\bar{k})$, with $\bar{k} = (K_B - \delta)$ and $\gamma = (\gamma_0 + \gamma_r)$, with $\gamma_r = (q_r - ik_r)$. The subscript r is used to emphasize the fact that the quantity under consideration is that due to the contribution from the random perturbation process.

Under the usual assumption that $\delta, g_0 \ll K_B, \bar{k} = K_B$, $(\Delta\gamma)$ can be expressed as

$$\Delta\gamma \approx [g_r^2 - k_r^2 - 2K_B k_r] - 2i(K_B g_r + g_r k_r). \quad (3.13b)$$

For an illustration, we shall consider the case where $g_r \ll k_r$. This is equivalent to assuming that the random perturbation process contributes mainly to the phase constant of the propagation constant γ . For this case Equation (3.13) is further simplified as

$$\Delta\gamma \approx -(2K_B k_r + k_r^2). \quad (3.14)$$

Upon substituting Equation (3.14) into Equation (3.12) we obtain

$$p_1 = 0 \quad (3.15a)$$

and

$$p_2 = -\rho_r, \quad (3.15b)$$

where

$$\rho_r = \frac{1}{2K_B} \int_{-\frac{L}{2}}^{\frac{L}{2}} (2K_B k_r + k_r^2) dz. \quad (3.16)$$

Consequently, Equation (3.8) through Equation (3.11) become

$$\bar{x}_0 = x_0 + A_2 \rho_r \quad (3.17)$$

$$\bar{y}_0 = y_0 - A_1 \rho_r \quad (3.18)$$

$$\bar{x} = x + B_2 \rho_r \quad (3.19)$$

$$\bar{y} = y - B_1 \rho_r . \quad (3.20)$$

Here the factors A_1 , A_2 , B_1 and B_2 are the function of x , y , x_0 and y_0 . The perturbation parameter ρ_r depends on the random variable k_r . There is a question of whether we should take the mean value of ρ_r or the rms value of ρ_r . For the illustration, we shall take the mean value and denote it with $\rho_0 = \bar{\rho}_r$. In order to calculate the mean value of the random variable ρ_r , which depends on the random variable k_r , we must specify the model of statistical process.

As is well-known that from the theory of statistics, a random variable ζ whose autocorrelation function is a decreasing exponential:

$$R_\zeta(\xi) = \sigma^2 e^{-\beta|\xi|} \quad (3.21)$$

is frequently a useful representation of random system disturbances. This autocorrelation function is representative of a first-order Gauss-Markov process (74). The statistics of this process are completely described by the autocorrelation function, given by Equation (3.21) in which the mean value is taken as zero. The expectation (or mean value) of the random variable ζ is defined as

$$\bar{\zeta} \equiv E\{\zeta\} = \int_{-\infty}^{\infty} \zeta G(\zeta) d\zeta, \quad (3.22)$$

where the normal probability density function $G(\zeta)$ has the

form of a Gaussian distribution.

The variance of ζ is defined as

$$\sigma^2 = \int_{-\infty}^{\infty} (\zeta - \bar{\zeta})^2 G(\zeta) d\zeta \quad (3.23)$$

or

$$\sigma^2 = E\{\zeta^2\} - [E\{\zeta\}]^2 \quad (3.24)$$

Suppose that k_r under consideration is a random variable in the stationary Gauss-Markov process. If we define a dimensionless random variable ζ as

$$\zeta = (k_r / K_B) \quad (3.25)$$

then Equation (3.16) becomes

$$\rho_r = \frac{K_B}{2} \int_{-\frac{L}{2}}^{\frac{L}{2}} (2\zeta + \zeta^2) dz \quad (3.26)$$

and the mean value $\bar{\zeta}$, and the mean square value $\overline{\zeta^2}$ can be calculated according to Equation (3.22). Since $\bar{\zeta}=0$ is assumed, and from Equation (3.24) $\overline{\zeta^2} = \sigma^2$, where σ is the standard deviation of the random variable ζ , the mean value of ρ_r can be easily calculated from Equation (3.26) to give

$$\rho_o = \bar{\rho}_r = \frac{1}{2} K_B L \sigma^2. \quad (3.27)$$

Taking the statistical average of Equation (3.17) through Equation (3.20) we obtain a set of equations involving \bar{x}_o , \bar{y}_o , \bar{x} , \bar{y} and $\bar{\rho}_r$. Upon specifying the value of ρ_o , the plots of \bar{x}_o , \bar{y}_o , \bar{x} , and \bar{y} vs. τ , were calculated and the results

are shown in Figure 7 through Figure 10.

For the weakly coupled case where $\tau^2 \ll 1$ and $\tau^2 \ll x_0^2$ (or $\kappa^2 \ll g^2$), from Figure 6, we observe that $y_0^2 \ll x_0^2$, $1 \ll x_0$. Equations 3.5 and 3.7 are reduced to give $A_1 \approx 1$, $A_2 = \frac{y_0}{x_0}$, $B_1 \approx -1$ and $B_2 \approx \frac{y_0}{x_0}$, so that

$$\bar{x}_0 = x_0 + \frac{y_0}{x_0} \rho_0 \quad (3.28a)$$

$$\bar{y}_0 = y_0 + \rho_0 \quad (3.28b)$$

$$\bar{x} = x + \frac{y_0}{x_0} \rho_0 \quad (3.29a)$$

$$\bar{y} = y + \rho_0. \quad (3.29b)$$

Here we observe that as $\tau \rightarrow 0$, $x_0 \rightarrow \infty$, $y_0 \rightarrow \frac{\pi}{2}$, $\bar{x}_0 \rightarrow x_0 \rightarrow \bar{x} \rightarrow x$, and $\bar{y}_0 \rightarrow \bar{y}$, which is consistent with the behavior shown in Figures 7 through 10.

On the other hand, for the strongly coupled case where $\tau^2 \gg 1$, and $\tau^2 \gg x_0^2$ (or $\kappa^2 \gg g^2$), once again from Figure 6 we observe that $y_0 > \tau$, $x_0^2 \ll y_0^2$, $x_0 \ll 1$, so that $A_1 = \frac{\tau^2}{2} - 1$, $A_2 = \frac{\tau^2}{y_0}$, $B_1 = \frac{-y_0}{y_0} = -\frac{\pi}{y_0}$ and $B_2 = \frac{y_0}{y_0} = \frac{\pi}{y_0}$. In this case, we have

$$\bar{x}_0 = x_0 + \frac{\tau^2}{y_0} \rho_0 \quad (3.30a)$$

$$\bar{y}_0 = y_0 + \left(1 - \frac{\tau^2}{y_0}\right) \rho_0 \quad (3.30b)$$

$$\bar{x} = x + \frac{y_0}{y_0} \rho_0 \quad (3.31a)$$

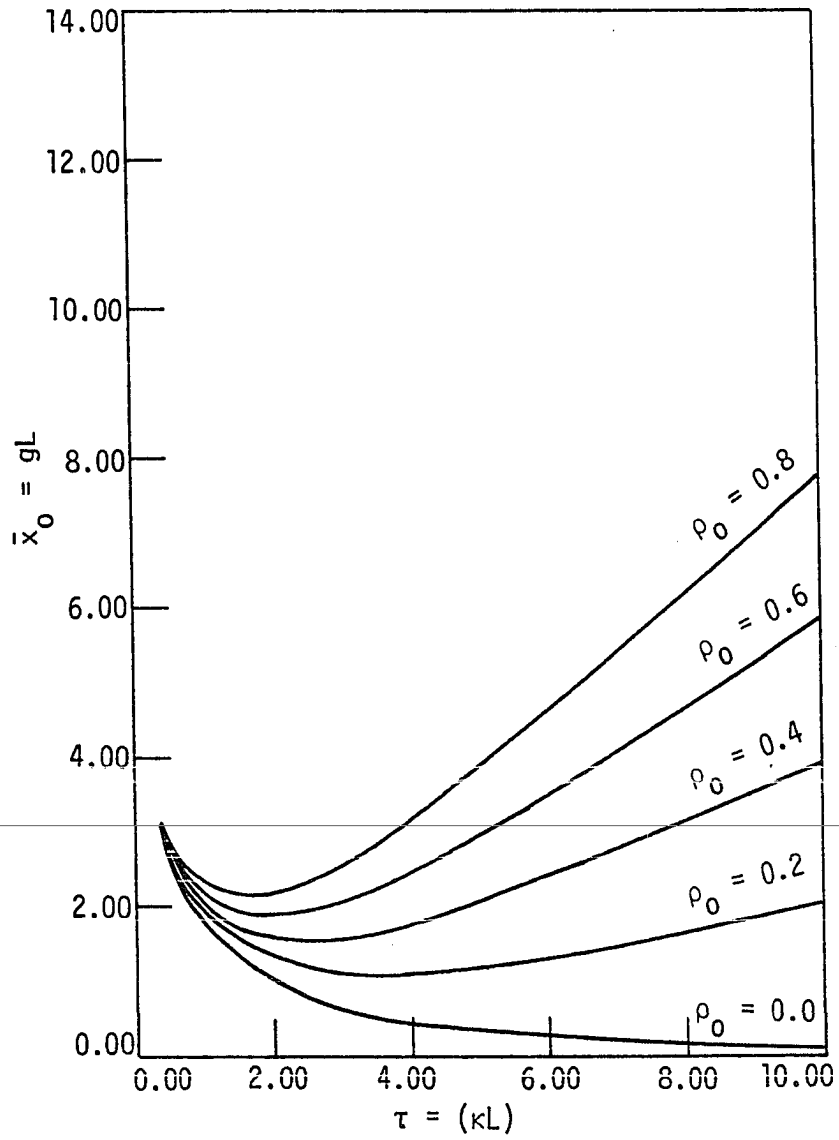


Figure 7. The variation of the gain parameter \bar{x}_0 with the coupling parameter τ for different values of the perturbation parameter ρ_0 .

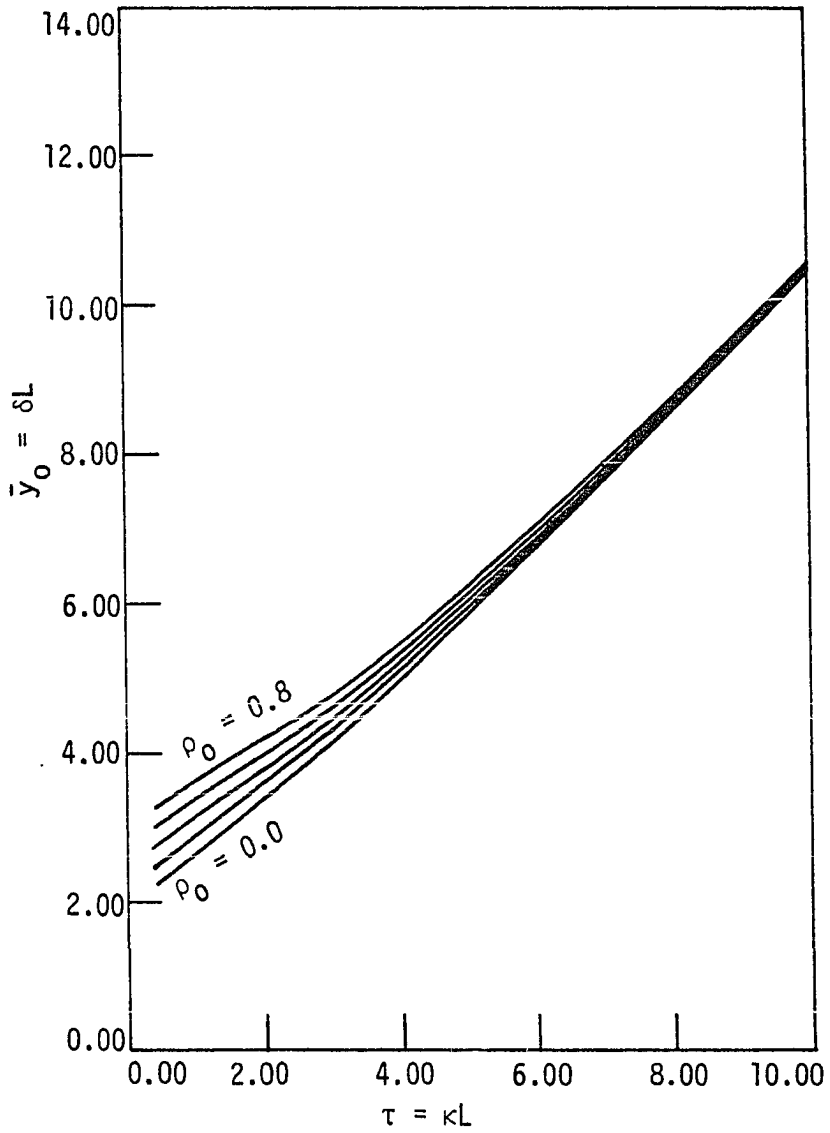


Figure 8. The variation of the phase parameter \bar{y}_0 with the coupling parameter τ for different values of the perturbation parameter ρ_0 .

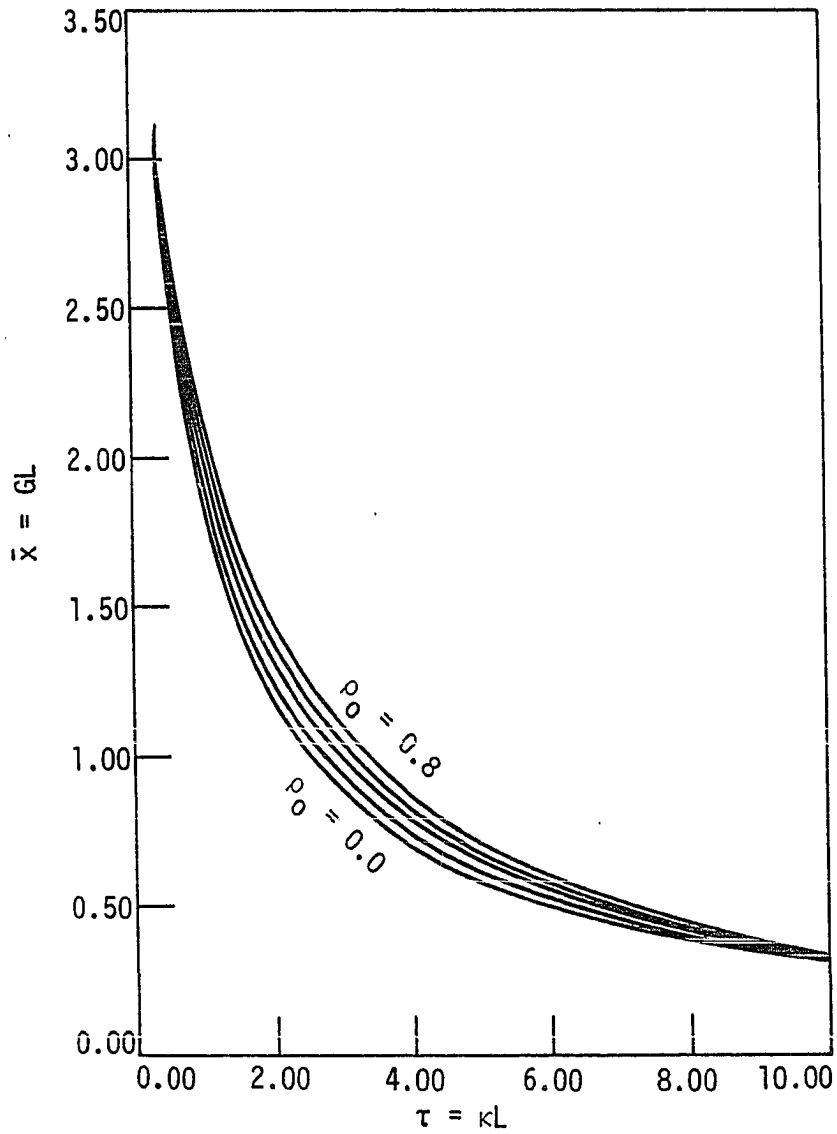


Figure 9. The variation of the perturbed effective gain parameter \bar{x} with the coupling parameter τ for different values of the perturbation parameter ρ_0

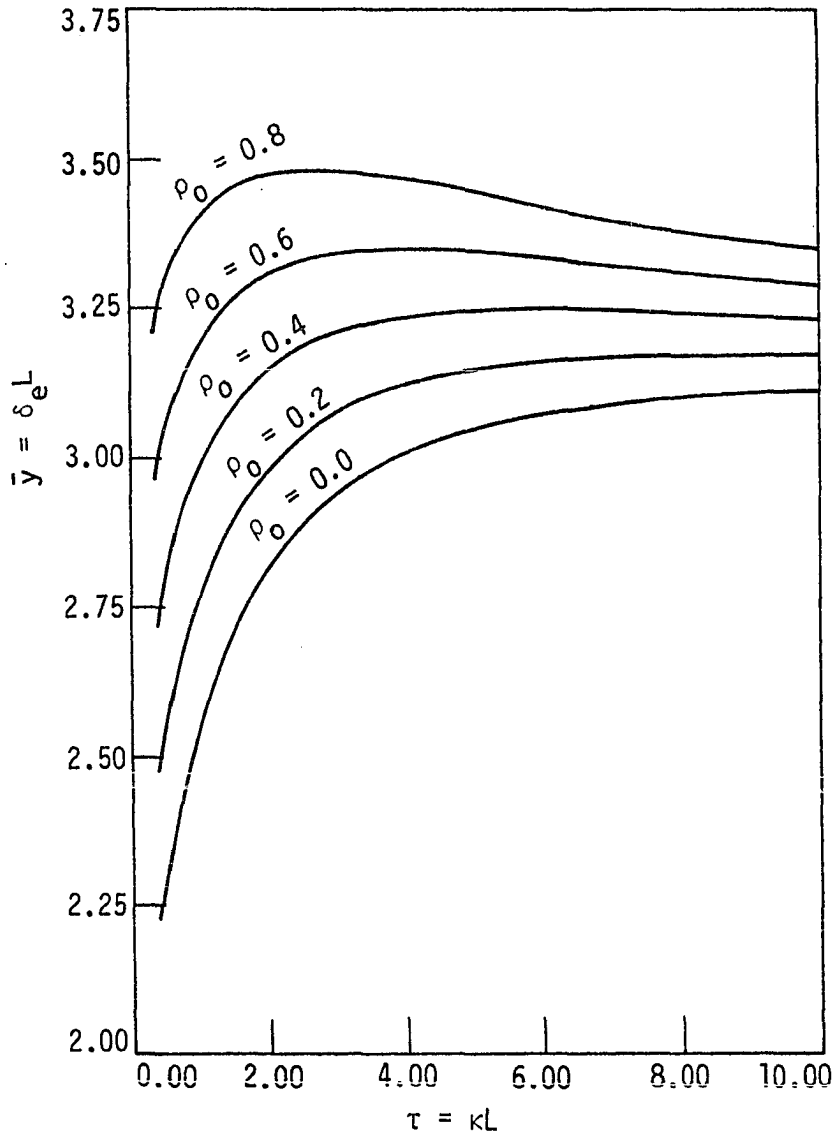


Figure 10. The variation of the perturbed effective phase parameter \bar{y} with the coupling parameter τ for different values of the perturbation parameter ρ_0

$$\bar{y} = y + \frac{y}{y_0} \rho_0. \quad (3.31b)$$

We note that as $\tau \rightarrow \infty$, $y \rightarrow \pi$, $y_0 \rightarrow \tau \rightarrow \infty$, $\bar{x}_0 \rightarrow (x_0 + \tau \rho_0)$, $\bar{y}_0 \rightarrow y_0$, $\bar{x} \rightarrow x_0$, and $\bar{y} \rightarrow y$, which is also shown in Figures 7 through 10.

IV. DISCUSSION OF RESULTS

The variation of the perturbed gain parameter $\bar{x}_0 = (gL)$ with the coupling parameter $\tau = (\kappa L)$ is illustrated in Figure 7 for different values of the perturbation parameter ρ_0 . It is observed that in the absence of the perturbation ($\rho_0=0$), $\bar{x}_0=x_0=(g_0L)$ decreases with τ monotonically, which suggests that the threshold gain, (i.e., the gain required for lasing) decreases as the coupling becomes stronger, which is to be expected. For a given value of τ , \bar{x}_0 increases with ρ_0 monotonically, which suggests that the required threshold gain increases as the degree of perturbation increases, which is also to be expected. The rate of increase of \bar{x}_0 with ρ_0 is small in the range of small τ , but it is large in the range of large τ . Furthermore, it is interesting to note that, for example, for the plot with $\rho_0 = 0.4$, \bar{x}_0 has its minimum value of 1.5 at $\tau \approx 2.5$, while for the case $\rho_0=0$, \bar{x}_0 decreases monotonically. For the case $\rho_0 = 0.6$, \bar{x}_0 has its minimum value of 1.75 at $\tau=2.0$. Thus as ρ_0 increases the position of the valley in the plot shifts to a lower τ and a higher \bar{x}_0 . The above observation tends to suggest that for a given value of ρ_0 , the required threshold gain would be minimum at a value of τ which is not necessarily large, in contrast to the case in which the perturbation is absent. We also observe that $\bar{x}_0 > x_0$, i.e., the perturbation gain parameter is

greater than its unperturbed counterpart. As $\tau \rightarrow 0$, $\bar{x}_0 \rightarrow x_0 \rightarrow \infty$, regardless of the value of ρ_0 , which suggests that the effect of the perturbation is insignificant when the coupling is so small that the required threshold gain has to be very large. On the other hand, in the range of large τ , the small perturbation can have greater effect on the required threshold gain.

The variation of the perturbed phase parameter $\bar{y}_0 = (\delta L)$ with coupling parameter τ is illustrated in Figure 8. It is observed that in the absence of perturbation, ($\rho_0 = 0$), $\bar{y}_0 = y_0 = (\delta_0 L)$ increases with τ monotonically, which suggests that the amount of detuning of the phase constant away from the Bragg wave number K_B increases with the strength of coupling. For a given value of τ , \bar{y}_0 increases monotonically with ρ_0 which suggests that the amount of detuning tends to increase with the degree of perturbation. The effect of the presence of the perturbation is larger in the region of small τ than that in the region of large τ . We observe that $\bar{y}_0 > y_0$, that is to say the perturbed phase parameter is greater than its unperturbed counterpart. As $\tau \rightarrow \infty$, $\bar{y}_0 \rightarrow y_0$, thus suggests that the effect of perturbation becomes insignificant as the degree of coupling is increased. However, the effect of perturbation can be significant if the coupling is very weak (see the behavior of \bar{y}_0 as $\tau \rightarrow 0$ in Figure 8).

The variation of perturbed effective gain parameter

$\bar{x} = (GL)$ with the coupling parameter τ is illustrated in Figure 9. It is observed that in the absence of perturbation $\bar{x} = x = (G_0 L)$ decreases with τ monotonically, and $x > x_0$, as seen in Figure 6. The behaviors of x and x_0 in the absence of perturbation are quite similar. The required threshold effective gain decreases with the degree of coupling, as is expected. In the presence of perturbation, since $\bar{x} > x$, the perturbed effective gain parameter is always greater than its unperturbed counterpart. We also observe that as $\tau \rightarrow 0$, $\bar{x} \rightarrow x$ and as $\tau \rightarrow \infty$ similarly $\bar{x} \rightarrow x$, whereas for the value of τ in the range $2 < \tau < 10$, \bar{x} increases significantly with ρ_0 . This suggests that unless either the extremely weakly coupled case or the extremely strongly coupled case are being considered, the effect of the perturbation in general, may not be negligible. In order to elaborate this aspect, a plot of the relative change in the gain parameter, $(\frac{\Delta x}{x})$, versus the coupling parameter τ , for different values of ρ_0 is shown in Figure 11, with the aid of Equation (3.19).

It is of interest to observe that the plots have peaks in the vicinity of $\tau \approx 3.0$. For example, at $\tau = 3.0$ an increase in the effective gain parameter is about 12.5% for $\rho_0 = 0.4$ and 25% for $\rho_0 = 0.8$. Thus the effect of the perturbation can be significant.

The variation of the perturbed effective phase parameter

$\bar{y} = (\delta_e L)$ with the coupling parameter τ is illustrated in Figure 10. It is observed that when $\rho_0 = 0$, $\bar{y} = y = (\delta_e L)$ increases monotonically with τ . In the range of small τ , y increases much more rapidly than in the range of large τ , and y tends to saturate as τ increases, then approach π . In the presence of the perturbation, $\bar{y} > y$ and \bar{y} increases with ρ_0 . For large values of ρ_0 , the plot of \bar{y} vs. τ possesses a peak, for example, at $\tau = 2.2$ for $\rho_0 = 0.8$. To see the relative change in y due to the presence of perturbation, we plot $(\frac{\Delta y}{y})$ vs. τ for different values of ρ_0 as shown in Figure 12. Since $(\frac{\Delta y}{y})$ decreases monotonically with τ , the effect of perturbation on the change in y is small in the range of large τ , whereas it can be significant when τ is small. This means that when the coupling is weak, the shift in the effective phase parameter can be significant. However, it is not very significant when the coupling is extremely strong. For example, at $\tau = 2.0$, $(\frac{\Delta y}{y})$ takes the values of 0.06 and 0.24 at $\rho_0 = 0.2$ and $\rho_0 = 0.8$ respectively.

It should be pointed out that the values of ρ_0 used in the illustrations of Figures 7 through 12 are reasonable. This can be seen as follows: Recall $\rho_0 = (\frac{1}{2} K_B L \sigma^2)$, where $K_B = (\frac{\pi}{a})$, with "a" being the spatial periodicity and L denotes the length of the periodic structure. Typical interaction lengths L are between 100 μm to 1 cm. Recently

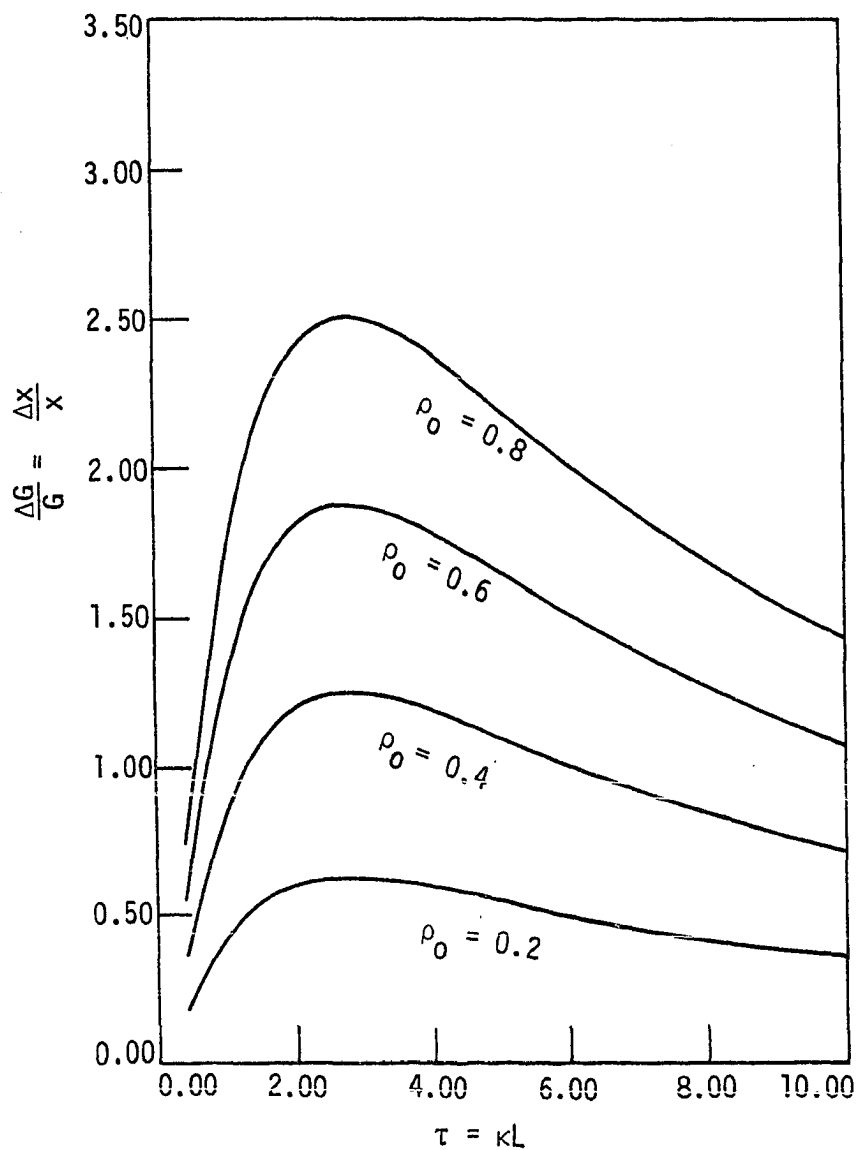


Figure 11. The variation of the relative change in the effective gain parameter; $(\Delta x/x)$ with the coupling parameter τ for different values of the perturbation parameter ρ_0

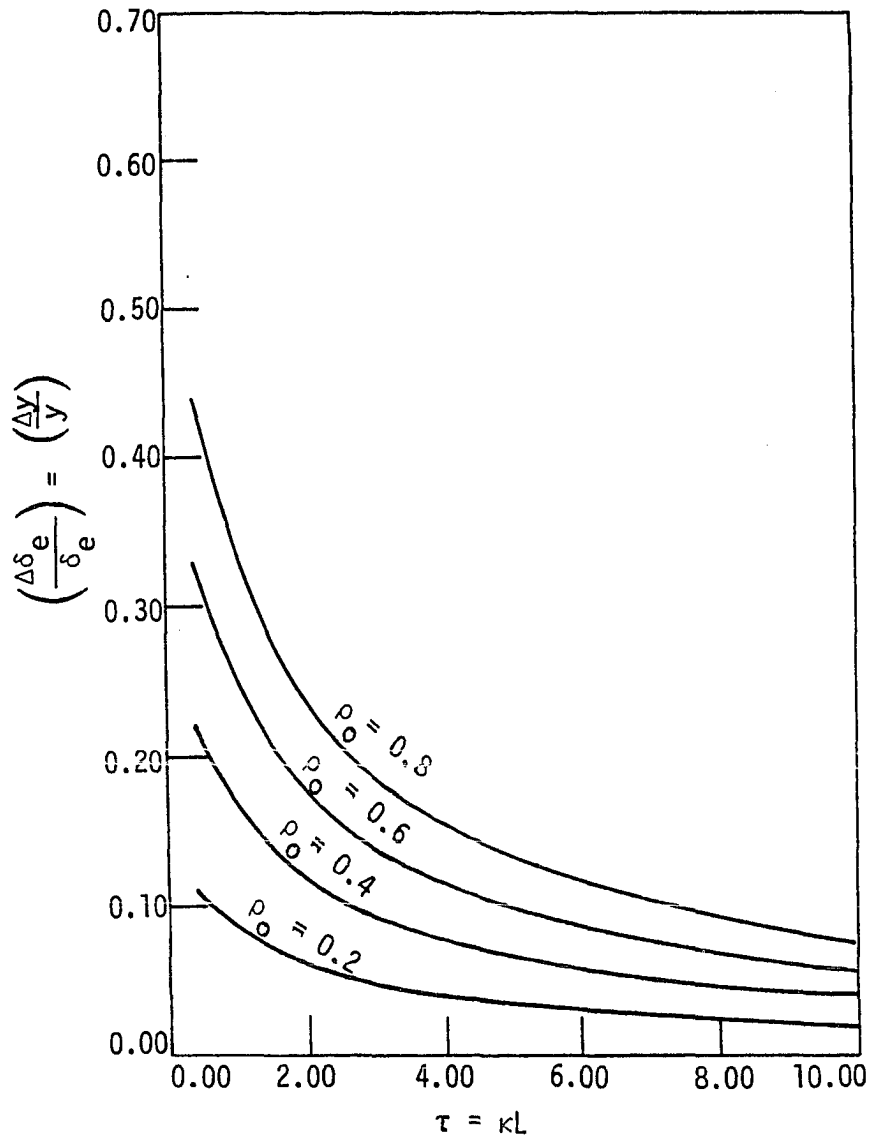


Figure 12. The variation of the relative change in the effective phase parameter; $(\Delta y/y)$ with the coupling parameter τ for different values of the perturbation parameter ρ_0

the distributed feedback operation of an AlGaAs laser has been demonstrated (75) in an electrically-pumped single-heterojunction GaAs laser at low temperature (77°K). In this device corrugations used were etched 1300Å deep and had a period of 3500Å. A grating of 0.36 μm periodicity produced by holographic means on an x-ray mask like that used by Bernacht and Smith (76). By taking "a" to be 0.3 μm, $(K_B L)$ takes the values in the range $10^3 \leq (K_B L) \leq 10^5$ when $10^{-4} \leq L \leq 10^{-2}$ m. Consequently, for $\rho_0 = 0.6$, the standard deviation $\sigma = (2 \frac{\rho_0}{K_B L})^{1/2}$ will take the values in the range, $3.5 \times 10^{-2} \geq \sigma \geq 3.5 \times 10^{-3}$.

It should be also be pointed out that in the present analysis only the lower order terms in the Maclaurin series expansion are considered by assuming the perturbation is sufficiently small. To study the case of larger perturbation, it is necessary to consider the higher order terms in the series. However, for such a case, the analysis would require the calculation of higher order statistical moments of a random variable which complicates the analysis.

In the present investigation, for the sake of simplicity, we assumed the perturbation parameter \tilde{p} is a purely imaginary quantity, i.e., $p_1 = 0$, and $p_2 = -\rho_r$, by assuming that $k_r \gg g_r$ in Equation (3.13b). This is equivalent to assuming

that the random perturbation process mainly affects the phase aspect of the propagation constant γ . However, it should be of interest to investigate the effect of g_r when it is not negligible in comparison with k_r . This is left for a future investigation.

In dealing with the perturbation parameter ρ_r we have a choice of whether to use the mean value or the rms value of the random variable ρ_r . For the sake of simplicity, the mean value was used, and the set of equations governing the mean perturbed gain parameters \bar{x}_0 , \bar{x} and the mean perturbed phase parameter \bar{y}_0 , \bar{y} are derived as a function of the mean value of ρ_r , (i.e., $\bar{\rho}_r = \rho_0$). If the rms value were to be taken then the rms value of the parameters x , x_0 , y , and y_0 must be considered in Equation (3.17) through Equation (3.20). In this case the analysis becomes considerably more complicated as indicated in Appendix A, since it would involve the evaluation of the rms value of ρ_r .

V. CONCLUDING REMARKS

In the present study the solution of a linear one-dimensional wave equation governing the electromagnetic fields of an optical wave in a periodic structure of the distributed feedback semiconductor laser is considered with the aid of the truncated Floquet-Bloch approach. The effect of a perturbation in the periodic structure such as an irregularity in the spatial periodicity or in the depth of corrugation of the periodic structure has been investigated.

First, the threshold condition for a perfectly periodic structure was derived by using the condition of the continuity of tangential components of electric and magnetic field intensities of the wave at the ends of the periodic interaction region. This unperturbed threshold condition is expressed in terms of a set of conveniently defined gain parameters; $x_0 = (g_0 L)$, $x = (G_0 L)$ and phase parameters; $y_0 = (\delta L)$, $y = (\delta_e L)$ and the coupling parameter $\tau = (\kappa L)$ as shown in Equations (2.102a-2.102d). Here we recall L denotes the length of the periodic structure, G_0 denotes the effective gain constant of the periodic structure, and $\delta_e = (K_B - K_0)$ is the amount of detuning of the phase constant K_0 away from the Bragg wave number K_B . g_0 denotes the gain constant in the absence of the periodic structure and $\delta = (K_B - \bar{k})$ is the counterpart of δ_e when the coupling is absent, i.e. the coupling coefficient $\kappa = 0$.

A small perturbation in the periodic structure is then introduced into the system. The effect of this perturbation on the threshold condition is examined with the aid of a truncated Maclaurin series and a first-order stationary Gauss-Markov process. The perturbation parameter $\bar{\rho}_r = \rho_0$ is introduced in the threshold condition. Using the derived perturbed threshold condition the changes in the gain parameters and in the phase parameters were investigated. The mean gain parameters \bar{x} , \bar{x}_0 and the mean phase parameters \bar{y} , and \bar{y}_0 are introduced into the discussion. The approximate expressions for \bar{x} , \bar{x}_0 , \bar{y} , and \bar{y}_0 as a function of τ and ρ_0 are obtained and calculated to investigate the significance of the effect of the perturbation.

The significant findings from the present study are described as follows:

1. The effective threshold gain constant required for lasing in the perturbed periodic structure, \bar{G} , increases with the perturbation parameter $\bar{\rho}_r$.
2. The effective detuning of the phase constant away from the Bragg wave number, $\bar{\delta}_e$, increases with $\bar{\rho}_r$.
3. The effect of perturbation on the effective gain constant is small when the device is operated in the regions of either very weak coupling or very strong coupling. However, for the intermediate value of τ , the effect of the perturbation on \bar{G} may be

quite significant. The plot of $(\Delta G/G)$ vs. τ , which shows the variation of the relative change in the effective gain constant with the coupling parameter, has a peak value of 0.125 at $(\kappa L) = \tau = 3.0$ when $\rho_r = 0.4$, and $(\Delta G/G)$ also increases with $\bar{\rho}_r$.

4. The effect of the perturbation on the effective phase constant δ_e is small when the device is operated in the region of strong coupling but is quite large when it is operated at the region of very weak coupling. $(\Delta\delta_e/\delta_e)$ decreases monotonically with τ but increases with $\bar{\rho}_r$. For example, when $\bar{\rho}_r=0.4$, $(\Delta\delta_e/\delta_e)$ takes the values of 0.09 and 0.05 at $(\kappa L) = 3.9$ and $(\kappa L) = 7.0$ respectively.

The result of the present study suggests that when the device is operated in the region of moderate coupling strength, say $0.1 < \tau < 10$ the effect of the perturbation on the effective gain and phase constant, G and δ_e of the periodic structure can be significant. In optimally designing a distributed feedback (DFB) laser it is important to determine the coupling coefficient and propagation constant. The coupling coefficient κ determines the minimum net gain and/or length of the structure, L , required to initiate laser operation (1, 77). A device operating at an overly large value of (κL) may also be suboptimal (77) so that it is undesirable. Since

a typical device is operated in the range of moderate values of (κL) , the effect of the perturbation under consideration cannot be neglected when it exists in the system.

Finally, it should be pointed out that the method of analyzing the perturbation effect in the periodic structure developed in the present study may also be applied to other types of semiconductor devices such as Bragg reflector (DBR) laser (78, 79) which employs the same type of periodic structure.

A. Suggestion for Further Studies

It will be desirable to extend the analysis to cover the case where the perturbation parameter $\tilde{p} = (p_1 + ip_2)$ is complex and the contribution of both g_r and k_r have to be taken into account.

Although the theoretical results reported in the present study are interesting, some sort of experimental verification indeed is desirable. For example, the assumption about the nature of the aperiodic perturbation, while reasonable, are unsubstantiated. One method of investigation would be to subject various distributed feedback structures to an external coherent sources and examine the scattering pattern. Since the scattering pattern represents the Fourier transform of the structure, some insight into the nature of

the perturbation might be gained. Another alternative would be to fabricate distributed feedback structures with intentionally induced imperfections and examine their gain and frequency characteristics. Unfortunately, other effects such as surface imperfection and deep traps may swamp changes induced by aperiodicity.

VI. REFERENCES

1. Kogelnik, H., and Shank, C. V. "Stimulated Emission in a Periodic Structure." Appl. Phys. Lett. 18 (February 1971):152-154.
2. Kogelnik, H., and Shank, C. V. "Coupled Wave Theory of Distributed Feedback Lasers." J. Appl. Phys. 43 (May, 1972):2327-2335.
3. Wang, S. "Principles of Distributed Feedback and Distributed Bragg-Reflector Lasers." IEEE J. Quantum Electron. QE-10, (April, 1974):413-427.
4. Wang, S. "Energy Velocity and Effective Gains." Appl. Phys. Lett. 26 (February, 1975):89-91.
5. Wang, S., Cordero, R. H. and Tseng, C. "Analysis of Distributed Feedback Bragg-Reflector Laser Structure by Method of Multiple Reflections." J. Appl. Phys. 45 (September, 1974):3975-3977.
6. Wang, S. and Tseng, W. "Analysis of Ring Distributed Feedback Lasers". J. Appl. Phys. 45 (September, 1974): 3978-3980.
7. Walpole, J. N., Calawa, A. R. Chinn, S. R. Grove, S. H., and Harman, T. C. "Distributed Feedback $\text{Pb}_{1-x}\text{Sn}_x\text{Te}$ Double Heterostructure Lasers." Appl. Phys. Lett. (September, 1976):307-309.
8. Okuda, M., Murata, K., and Oonaka, K. "Mode Selectivity of a Distributed Bragg-Reflector Laser with Optical Loss in the Corrugated Waveguide." Japan. J. Appl. Phys. 14 (November, 1975):1856-1859.
9. Iga, K. and Kawabata, K. "Active Bragg Reflector and its Application to Semiconductor Lasers." Japan J. Appl. Phys. 14 (March 1975):427-428.
10. Reinhart, F. K., Logan, R. A. and Shank, C. V. " $\text{GaAsAl}_x\text{Ga}_{1-x}\text{As}$ Injection Lasers with Distributed Bragg Reflectors." Appl. Phys. Lett. 27 (July, 1975): 45-48.

11. Streifer, W., Burnham, R. D., and Scifres, D. R.
"Coupling Coefficients and Propagation Constants in Guided Wave Distributed Feedback Lasers." J. Appl. Phys. 46 (February, 1975):946-948.
12. Scifres, D. R., Burnham, R. D., and Streifer, W.
"Highly Collimated Laser Beams from Electrically Pumped SH GaAs/GaAlAs Distributed Feedback Lasers." Appl. Phys. Lett. 26 (January, 1975):48-50.
13. Burnham, R. D., Scifres, D. R. and Streifer, W.
"Distributed Feedback Buried Heterostructure Diode Laser." Appl. Phys. Lett. 29, (September, 1976): 287-289.
14. Anderson, D. B., August, R. R., and Coker, J. E.
"Distributed Feedback Double Heterostructure GaAs Injection Laser with Fundamental Grating." Appl. Optics 13 (December, 1974):2742-2745.
15. Okuda, J., Murata, K., and Oonaka, K. "Optimum Design of a Distributed Bragg Reflector Laser with Optical Loss in the Corrugated Waveguide." Optical Comm. 16 (January, 1976):30-32.
16. Scifres, D. R., Burnham, R. D., and Streifer, W.
"Distributed-Feedback Single Heterojunction GaAs Diode Laser." Appl. Phys. Lett. 25 (August, 1974):203-206.
17. Grove, A. S. Physics and Technology of Semiconductor Devices. New York: Wiley, 1967.
18. Miller, S. E. "A Survey of Integrated Optics." IEEE J. Quantum Electron. QE-8 (February, 1972):199-205.
19. Somekh, S., Casey, H. C., and Ilegems, M. "Preparation of High-Aspect Ratio Periodic Corrugations by Plasma and Ion Etching." Appl. Optics, 15 (August, 1976):1905-1906.
20. Shank, C. V. and Schmidt, R. V. "Optical Technique for Producing 0.1 μ Periodic Surface Structures." Appl. Phys. Lett., 23, (August, 1973):154-155.
21. Tsang, W., and Wang, W. "Grating Masks Suitable for Ion Beam Machining and Chemical Etching." Appl. Phys. Lett. 25 (October, 1974):415-418.

22. Smith, H. I. "Fabrication Techniques for Surface-Acoustic Wave and Thin Film Optical Devices." Proc. IEEE 62 (October, 1974):1361-1387.
23. Marcuse, D. "Mode Conversion Caused by Surface Imperfections of a Dielectric Slab Waveguide." Bell Syst. Tech. J. 48 (1969):3187-3215.
24. Yariv, A. "Coupled-Mode Theory for Guided Wave Optics." IEEE J. Quantum Electron. QE-9 (1973):919-933.
25. Streifer, W., Scifres, D. R., and Burnham, R. D. "Coupled Wave Analysis of DFB and DBR Lasers." IEEE J. Quantum Electron. QE-13, (1977):134-141.
26. Cordero, R., and Wang, S. "Threshold Condition for Thin-Film DFB Lasers." Appl. Phys. Lett. 24 (1974):474-476.
27. Wang, S. "Thin Film Bragg Lasers for Integrated Optics." Wave Electronics, 1, (1974):31-59.
28. Wang, S. "Proposal of Periodic Layered Waveguide Structure for Distributed Lasers." J. Appl. Phys. 44, (1973):767-780.
29. Wang, S. and Shen, S. "Two-dimensional Distributed-Feedback Lasers and their Applications." Appl. Phys. Lett. 22, (1973):460-462.
30. DeWames, R. E., and Hall, W. F. "Conditions for Laser Oscillation in Distributed-Feedback Waveguides." Appl. Phys. Lett. 23 (1973):28-30.
31. Yariv, A., and Gover, A. "Equivalence of Coupled-Mode and Floquet-Bloch Formalism in Periodic Optical Waveguides." Appl. Phys. Lett. 26 (1975):537.
32. Einstein, A. "On the Quantum Theory of Radiation." Laser Theory. Pp. 5-21, Edited by Frank S. Barnes, New York: IEEE Press, 1972.
33. Lengyel, B. A. Lasers. New York: Wiley, 1971.
34. Sargent, M., Scully, M. O., and Lamb, W. E., Laser Physics. London: Addison Wesley, 1974.

35. Gooch, C. H. "Properties of Gallium Arsenide p-n Junction Lasers." Gallium Arsenide Lasers, pp. 81-132, Edited by C. H. Gooch. London: Wiley-Interscience, 1969.
36. Rieck, H. Semiconductor Lasers. London: MacDonald, 1970.
37. Gooch, C. H. Injection Electroluminescent Devices. London: Wiley, 1973.
38. Pankove, J. I. Optical Processes in Semiconductors. Englewood Cliffs: Prentice-Hall, 1971.
39. Nathan, M. E. "Semiconductor Lasers." Proc. IEEE 54 (October, 1966):1276-1290.
40. Burns, G. and Nathan, M. E. "P-N Junction Lasers." Proc. IEEE 52 (October, 1964):770-794.
41. Basov, N. G., Vul, B. M. and Popov, Y. M. "Quantum Mechanical Semi-Conductor Generations and Amplifiers of Electromagnetic Oscillations." Soviet Phys. JETP 10 (February, 1960):416.
42. Kroemer, H. "A Proposed Class of Heterostructure Injection Lasers." Proc IEEE 51 (December, 1963):1782-1783.
43. Panish, M. B. "Heterostructure Injection Lasers." Proc. IEEE 64 (October, 1976):1512-1540.
44. Panish, M. B. "Heterostructure Injection Lasers." IEEE MTT Trans. MTT-23 (January, 1975):20-30.
45. Casey, H. C., Jr. and Panish, M. B. "Composition Dependence of the $\text{Ga}_{1-x}\text{Al}_x\text{As}$ Direct and Indirect Energy Gaps." J. Appl. Phys. 40 (November 1969):4910-4912.
46. Alferov, Z. I. "Possible Development of a Rectifier for Very High Current Densities on the Basis of a P-i-n (p-n-n^+ , n-p-p^+) Structure with Heterojunctions." Sov. Phys. Semicond. 1 (September, 1967):358-360.
47. Schul, G. and Mischel, P. " $\text{Ga}_x\text{In}_{1-x}\text{P}\text{Ga}_y\text{Al}_{1-y}\text{As}$ Heterojunction Close-Confinement Injection Laser." Appl. Phys. Lett. 27 (April, 1975):394-395.

48. Rakshit, S., Biswas, S. N., and Chakravarti, A. N. "Effect of Wave Confinement in Heterostructure Injection Lasers." Int. J. Electron 36 (May, 1974):593-600.
49. Panish, M. B., Casey, H. C., Simski, S., and Foy, P. W. "Reduction of Threshold Current Density in GaAs-Al_xGa_{1-x}As Heterostructure Lasers by Separate Optical and Carrier Confinement." Appl. Phys. Lett. 22 (June, 1973):590-591.
50. Ikegami, T. "Reflectivity of Mode at Facet and Oscillation Modes in Double Heterostructure Injection Lasers." IEEE J. Quantum Electron QE-8, (June, 1972): 470-476.
51. Born, M., and Wolf, E. Principles of Optics. Oxford: Pergamon Press, 1975.
52. Harrington, R. F. Time Harmonic Electromagnetic Fields. New York: McGraw-Hill, 1961.
53. Marcuse, D. Light Transmission in Optics. New York: Van Nostrand-Reinhold, 1972.
54. Moss, T. S. Optical Properties of Semi-Conductors. New York: Butterworth, 1959.
55. Sze, S. M. Physics of Semiconductor Devices. New York: Wiley-Interscience, 1969.
56. Hayashi, E., and Panish, M. B. "GaAsGaAl_{1-x}As_x Heterostructure Injection Lasers which Exhibit Low Threshold at Room Temperature." J. Appl. Phys. 41 (January, 1973): 150-163.
57. Casey, H. C., and Panish, M. B. "Influence of Al_xGa_{1-x}As Layer Thickness on Threshold Current Density and Differential Quantum Efficiency for GaAsAl_xGa_{1-x}As Double Heterostructure Lasers." J. Appl. Phys. 46 (March, 1975):1393-1395.
58. Hayashi, I., Panish, M. B., Foy, P. W. and Sumski, S. "Junction Lasers which Operate Continuously at Room Temperature." Appl. Phys. Lett. 17, (August, 1970): 109-111.

59. Poali, T. L., and Ripper, J. E. "Optical Properties of Junction Lasers Operating Continuously at Room Temperature." Appl. Phys. Lett. 18 (May, 1971):466-468.
60. Yonezu, H., Sakoma, I., and Kobayashki, K. "GaAs-Al_xGa_{1-x}As Double Heterostructure Planar Laser." Japan J. Appl. Phys. 12 (October, 1973): 1585-1592.
61. Chernov, L. A. Wave Propagation in a Random Medium. New York: McGraw-Hill, 1960.
62. Tatarski, V. I. Wave Propagation in a Turbulent Medium. New York: McGraw-Hill. 1961.
63. Ishimaru, A. "Theory and Application of Wave Propagation and Scattering in Random Media." Proc. IEEE 65 (July 1977):1030-1061.
64. Brayer, K. Data Communication in Fading Channels. New York: IEEE Press, 1975.
65. David, P. and Voge, J. Propagation of Waves. Oxford: Pergamon Press, 1969.
66. DuCastel, F. Tropospheric Radiowave Propagation Beyond the Horizon. Oxford: Pergamon Press, 1966.
67. Ramachandran, G. N., and Srinivasan, R. Fourier Methods in Crystallography. New York: Wiley, 1970.
68. Kakudo, M., and Kasai, N. X-ray Diffraction by Polymers. Tokyo: Kodansha Ltd., 1972.
69. Kittel, C. Introduction to Solid State Physics. New York: Wiley, 1971.
70. Brillouin, L. Wave Propagation in Periodic Structures. New York: Dover, 1953.
71. Elachi, C. "Waves in Active and Passive Periodic Structures: A Review." Proc. IEEE, 64 (December, 1976): 1666-1698.

72. Peng, S. T., Tamir, T. and Bertoni, H. L. "Theory of Periodic Waveguides." IEEE MTT Trans. MTT-23, (January, 1975):123-133.
73. Okuda, M., and Kubo, K. "Analysis of the Distributed Bragg-Reflector Laser of Asymmetrical Geometry." Japan J. Appl. Phys. 14 (June, 1975):855-860.
74. Gelb, A. Applied Optimal Estimation. Cambridge: The MIT Press, 1974.
75. Kogelnik, H. "An Introduction to Integrated Optics." IEEE Trans. MTT-23, (January, 1975):2-16.
76. Bernacht, S. E., and Smith, H. I. "X-ray lithography applied to Silicon Device Fabrication." Proc. of 6th Conf. on Elect. and Ion Beam Science and Technology. San Francisco, May, 1974.
77. Chinn, S. R. "Effects of Mirror Reflectivity in a Distributed Feedback Laser." IEEE J. Quantum Electron QE-9 (1973):574-580.
78. Tsang, W. T., and Wang, S. "GaAs-Ga_{1-x}Al_xAs Double-Heterostructure injection Lasers with Distributed Bragg Reflectors." Appl. Phys. Lett. 28 (May, 1976): 596-598.
79. Yen, H. W., Samid, W. Ng, and Yariv, A. "GaAs Distributed Bragg Reflector Lasers." Optics Communication 17 (June, 1976):213-218.
80. Papaulis, A. Probability, Random Variables and Stochastic Processes. New York: McGraw-Hill. 1965.
81. Cooper, G. R. and McGillum, C. D. Probabilistic Methods of Signal and System Analysis. New York: Holt, Rinehart and Winston, 1971.

VII. ACKNOWLEDGMENTS

To Dr. H. C. Hsieh I extend my sincerest thanks for his invaluable assistance and support throughout my graduate program.

To my wife Olga must go my deepest appreciation for her encouragement and patience,

VIII. APPENDIX

The introduction of perturbation into the system produced a change in the propagation parameter as shown in Equation (3.2a) for $\tilde{W}(\tilde{p})$ and Equation (3.2b) for $\tilde{w}(\tilde{p})$:

$$\tilde{W} = \tilde{W}_0 + \Delta\tilde{W} \quad (\text{A.1a})$$

$$\tilde{w} = \tilde{w}_0 + \Delta\tilde{w} \quad (\text{A.1b})$$

where

$$\Delta\tilde{W} = \left. \frac{d\tilde{W}}{d\tilde{p}} \right|_{\tilde{p}=0} \tilde{p} \quad \text{and} \quad \tilde{W}_0 = (x+iy) \quad (\text{A.2a})$$

$$\Delta\tilde{w} = \left. \frac{d\tilde{w}}{d\tilde{p}} \right|_{\tilde{p}=0} \tilde{p} \quad \text{and} \quad \tilde{w}_0 = (x_0+iy_0). \quad (\text{A.2b})$$

The perturbation parameter \tilde{p} is complex in general and is taken as a random variable. By writing $\tilde{p}=p_1+ip_2$ (A.3)

$$\left. \frac{d\tilde{W}}{d\tilde{p}} \right|_{\tilde{p}=0} = B_1+iB_2 \quad (\text{A.4})$$

and

$$\left. \frac{d\tilde{w}}{d\tilde{p}} \right|_{\tilde{p}=0} = A_1+iA_2. \quad (\text{A.5})$$

we have from Equation (A.4)

$$\Delta x = (B_1 p_1 - B_2 p_2) \quad (\text{A.6a})$$

and

$$\Delta y = (B_2 p_1 + B_1 p_2). \quad (\text{A.6b})$$

From Equation (A.5)

$$\Delta x_0 = (A_1 p_1 - A_2 p_2) \quad (\text{A.7a})$$

and

$$\Delta y_0 = (A_2 p_1 + A_1 p_2). \quad (\text{A.7b})$$

Here the coefficients, A_1 , A_2 , B_1 and B_2 are the values evaluated for the case of absence of perturbation and are independent of p_1 and p_2 . On the other hand, p_1 and p_2 are random variables. Consequently the quantities Δx , Δy , Δx_0 , and Δy_0 are also random variables.

Since $x_0 = (gL)$, and $y_0 = (\delta L)$, for example, the changes in the gain constant Δg and in the phase constant $\Delta \delta$ can be investigated. However, a question arises as to whether the mean value, $(E\{\Delta g\} = \overline{\Delta g})$ or the rms value $(E\{g^2\} = \overline{(\Delta g)^2})$ should be used. Here $E\{ \}$ denotes the expectation operator, and the averaging process depends upon the model of the probability density function assumed.

For example, by applying the expectation operator on Equation (A.7) and recalling $E\{p_1 p_2\} = 0$, we have

$$E\{\Delta x_0\} = \overline{\Delta x_0} = A_1 \bar{p}_1 - A_2 \bar{p}_2 \quad (\text{A.8a})$$

$$E\{\Delta y_0\} = \overline{\Delta y_0} = A_2 \bar{p}_1 + A_1 \bar{p}_2 \quad (\text{A.8b})$$

$$E\{(\Delta x_0)^2\} = \overline{(\Delta x_0)^2} = A_1^2 \overline{p_1^2} + A_2^2 \overline{p_2^2} \quad (\text{A.9a})$$

$$E\{(\Delta y_0)^2\} = \overline{(\Delta y_0)^2} = A_2^2 \overline{p_1^2} + A_1^2 \overline{p_2^2}. \quad (\text{A.9b})$$

The variance may be computed as

$$\begin{aligned} \sigma_{x_0}^2 &= E\{(\Delta x_0)^2\} - [E\{\Delta x_0\}]^2 \\ &= \overline{(\Delta x_0)^2} - (\overline{\Delta x_0})^2 \\ &= A_1^2 \sigma_{p_1}^2 + A_2^2 \sigma_{p_2}^2 + 2A_1 A_2 E\{p_1\} E\{p_2\}. \end{aligned} \quad (\text{A.10a})$$

Similarly:

$$\sigma_{y_0}^2 = A_1^2 \sigma_{p_1}^2 + A_2^2 \sigma_{p_2}^2 - 2A_1 A_2 E\{p_1\} E\{p_2\} \quad (\text{A.10b})$$

In the present study p_1 is taken as zero. The parameter η_r , given by Equation (2.79), was expressed in terms of the perturbation parameter $p_2 = -\rho_r$ as in Equation (3.16), in which k_r is treated as a random variable so that the perturbation parameter ρ_r or η_r is also a random variable.

We are now faced with the task of statistically describing a function of the form

$$\eta = \int_0^L \varepsilon(z) dz, \quad (\text{A.11})$$

$$\text{where } \varepsilon(z) = Ak(z) + Bk^2(z). \quad (\text{A.12})$$

and $k(z)$ is zero mean, first order Gauss-Markov process

defined by its auto-correlation function

$$R_k(\xi) = E\{k(z)k(z+\xi)\}. \quad (\text{A.13})$$

Recall now (80, 81)

$$R_y(\xi) = \int_0^\infty \int_0^\infty R_x(\lambda_2 - \lambda_1 - \xi) h(\lambda_1) h(\lambda_2) d\lambda_1 d\lambda_2 \quad (\text{A.14})$$

$$y(z) = \int_0^\infty x(z-\lambda) h(\lambda) d\lambda \quad (\text{A.15})$$

Clearly, for the function described in Equation (A.11)

$$h(\lambda) = u(\lambda) - u(\lambda-L) \quad (\text{A.16})$$

$$u(\lambda) = \begin{cases} 0 & \lambda < 0 \\ 1 & \lambda \geq 0 \end{cases} \quad (\text{A.17})$$

Use of Equation (A.4) requires the autocorrelation function for ε :

$$R_\varepsilon = A^2 R_k + B^2 R_{k^2} + 2ABR_{kk^2} \quad (\text{A.18})$$

$$\begin{aligned} R_{kk^2} &= E\{k(z)k^2(z+\xi)\} = 0 \\ &= E\{k(z+\xi)k^2(z)\} = 0 \end{aligned}$$

We now require

$$R_{k^2}(\xi) = E\{k^2(z)k^2(z+\xi)\}. \quad (\text{A.19})$$

Recall for two jointly normal, zero mean random variables

$$E\{x^2y^2\} = E\{x^2\}E\{y^2\} + 2E^2\{xy\}. \quad (\text{A.20})$$

Then

$$R_{k^2}(\xi) = E\{k^2(z)\}E\{k^2(z+\xi)\} + 2E^2\{k(z)k(z+\xi)\} \quad (\text{A.21})$$

Recall k is stationary; hence

$$E\{k^2(z)\} = E\{k^2(z+\xi)\} = R_k(0). \quad (\text{A.22})$$

Also note

$$E\{k(z)k(z+\xi)\} = R_k(\xi). \quad (\text{A.23})$$

Hence

$$R_{k^2}(\xi) = R_k^2(0) + 2R_k^2(\xi) \quad (\text{A.24})$$

and

$$R_\epsilon(\xi) = R_1(\xi) + R_2(\xi) + R_3(\xi) \quad (\text{A.25})$$

where

$$R_1 = B^2R_k^2(0)$$

$$R_2 = A^2R_k(\xi)$$

$$R_3 = 2B^2R_k^2(\xi).$$

We may now evaluate $R_\eta(\xi)$ using Equations (A.14) and (A.15), for representative $R_k(\xi)$.

Let

$$R_k(\xi) = \frac{\beta s_0}{2} \exp(-\beta|\xi|) \quad (\text{A.26})$$

where

$$\beta \ll K_B$$

Then

$$\begin{aligned} R_1(\xi) &= B^2 \left(\frac{\beta s_0}{2}\right)^2 \\ R_2(\xi) &= A^2 \left(\frac{\beta s_0}{2}\right) \exp[-\beta|\xi|] \\ R_3(\xi) &= 2B^2 \left(\frac{\beta s_0}{2}\right)^2 \exp[-2\beta|\xi|]. \end{aligned} \quad (\text{A.27})$$

Note that Equation (A.14) is linear in R so that $R_\eta(\xi)$ may be computed term by term. Examining these in order of complexity, we first consider the contribution of the constant term.

$$R_{1\eta}(\xi) = \int_0^\infty \int_0^\infty B^2 \left(\frac{\beta s_0}{2}\right)^2 [u(\lambda_1) - u(\lambda_1 - L)] [u(\lambda_2) - u(\lambda_2 - L)] d\lambda_1 d\lambda_2 \quad (\text{A.28})$$

$$= B^2 \left(\frac{\beta s_0}{2}\right)^2 \int_0^L \int_0^L d\lambda_1 d\lambda_2 \quad (\text{A.29})$$

$$= B^2 \left(\frac{\beta s_0}{2}\right)^2 L^2 \quad (\text{A.30})$$

The next contribution is from $R_k(\xi)$.

$$R_{2\eta} = \int_0^\infty \int_0^\infty A^2 \left(\frac{\beta s_0}{2}\right) \exp(-\beta|\lambda_2 - \lambda_1 - \xi|) [u(\lambda_1) - u(\lambda_1 - L)] [u(\lambda_2) - u(\lambda_2 - L)] d\lambda_1 d\lambda_2 \quad (\text{A.31})$$

First integrating with respect to λ_2 ; note that $\exp(-\beta|\lambda_2 - \lambda_1 - \xi|)$ has discontinuous derivatives at the origin and must be split.

$$\exp[-\beta|\lambda_2 - \lambda_1 - \xi|] = \begin{cases} \exp[-\beta(\lambda_2 - \lambda_1 - \xi)] & \text{for } \lambda_2 > \lambda_1 + \xi \\ \exp[\beta(\lambda_2 - \lambda_1 - \xi)] & \text{for } \lambda_2 \leq \lambda_1 + \xi \end{cases} \quad (\text{A.32})$$

Since the autocorrelation function is even, we assume positive ξ and invoke symmetry to complete $R(\xi)$.

Therefore:

$$\begin{aligned} & \int_0^\infty \exp(-\beta|\lambda_2 - \lambda_1 - \xi|) [u(\lambda_2) - u(\lambda_2 - L)] d\lambda_2 \quad (\text{A.33}) \\ &= \int_0^{\lambda_1 + \xi} \exp[\beta(\lambda_2 - \lambda_1 - \xi)] [u(\lambda_2) - u(\lambda_2 - L)] d\lambda_2 + \\ & \quad \int_{\lambda_1 + \xi}^\infty \exp[-\beta(\lambda_2 - \lambda_1 - \xi)] [u(\lambda_2) - u(\lambda_2 - L)] d\lambda_2 \end{aligned}$$

Each of these integrals must again be split.

$$\begin{aligned} & \int_0^{\lambda_1 + \xi} \exp[\beta(\lambda_2 - \lambda_1 - \xi)] [u(\lambda_2) - u(\lambda_2 - L)] d\lambda_2 \\ &= \begin{cases} \int_0^{\lambda_1 + \xi} \exp[\beta(\lambda_2 - \lambda_1 - \xi)] d\lambda_2, & \lambda_1 + \xi < L \\ \int_0^L \exp[\beta(\lambda_2 - \lambda_1 - \xi)] d\lambda_2, & \lambda_1 + \xi \geq L \end{cases} \quad (\text{A.34}) \end{aligned}$$

$$\begin{aligned}
 & \int_{\lambda_1+\xi}^{\infty} \exp[-\beta(\lambda_2-\lambda_1-\xi)] [u(\lambda_2)-u(\lambda_2-L)] d\lambda_2 \\
 &= \begin{cases} \int_{\lambda_1+\xi}^L \exp[-\beta(\lambda_2-\lambda_1-\xi)] d\lambda_2, & \lambda_1+\xi < L \\ 0 & \lambda_1+\xi \geq L \end{cases} \quad (\text{A.35})
 \end{aligned}$$

Completing the solution of these intermediate integrals gives:

$$\begin{aligned}
 & \int_0^{\infty} R_k(\lambda_2-\lambda_1-\xi) [u(\lambda_2)-u(\lambda_2-L)] d\lambda_2 = \\
 & \begin{cases} \frac{1}{\beta} \{2-\exp[-\beta(\lambda_1+L)]-\exp[-\beta(L-\lambda_1-\xi)]\}, & \lambda_1+\xi < L \\ \frac{1}{\beta} \{\exp[\beta(L-\lambda_1-\xi)]-\exp[-\beta(\lambda_1+\xi)]\}, & \lambda_1+\xi \geq L \end{cases} \quad (\text{A.36})
 \end{aligned}$$

Hence,

$$\begin{aligned}
 R_{2\eta}(\xi) &= \frac{A^2 \beta s_0}{2} \left\{ \int_0^{L-\xi} I_1 [u(\lambda_1)-u(\lambda_1-L)] d\lambda_1 \right. \\
 & \quad \left. + \int_{L-\xi}^{\infty} I_2 [u(\lambda_1)-u(\lambda_1-L)] d\lambda_1 \right\} \quad (\text{A.37})
 \end{aligned}$$

where

$$I_1 = \frac{1}{\beta} \{2-\exp[-\beta(\lambda_1+L)]-\exp[-\beta(L-\lambda_1-\xi)]\} \quad (\text{A.38a})$$

$$I_2 = \frac{1}{\beta} \{\exp[\beta(L-\lambda_1-\xi)]-\exp[-\beta(\lambda_1+\xi)]\}. \quad (\text{A.38b})$$

Evaluating the integrals gives:

$$\int_0^{L-\xi} I_1 [u(\lambda_1) - u(\lambda_1 - L)] d\lambda_1$$

$$= \frac{2}{\beta}(L-\xi) + \frac{1}{2} \{ \exp(-\beta L) - \exp(-\beta \xi) + \exp[-\beta(\xi-L)] - 1 \}$$
(A.39)

$$\int_{L-\xi}^{\infty} I_2 [u(\lambda_1) - u(\lambda_1 - L)] d\lambda_1$$

$$= \frac{1}{\beta^2} \{ 1 - \exp(-\beta \xi) + \exp[-\beta(L+\xi)] - \exp(-\beta L) \}$$
(A.40)

Hence,

$$R_{2\eta}(\xi) = A^2 s_o \left((L-\xi) + \frac{1}{2\beta} \{ \exp[-\beta(L-\xi)] + \exp[-\beta(L+\xi)] - 2 \exp[-\beta \xi] \} \right),$$

for $L \geq \xi > 0$

(A.41a)

and by symmetry

$$R_{2\eta}(\xi) = A^2 s_o \left[(L+\xi) + \frac{1}{2\beta} \{ \exp[-\beta(L+\xi)] + \exp[-\beta(L-\xi)] - 2 \exp[\beta \xi] \} \right], \text{ for } -L < \xi < 0.$$
(A.41b)

Similar analysis for $R_{3\eta}$ gives

$$\begin{aligned}
 R_{3\eta}(\xi) &= \frac{B^2 s_0^2}{2} [\beta(L-\xi) + \frac{1}{4} \{ \exp[-2\beta(L-\xi)] + \exp[-2\beta(L+\xi)] \\
 &\quad - 2 \exp[-2\beta\xi] \}], \quad L \leq \xi \leq 0 \\
 &= \frac{B^2 s_0^2}{2} [\beta(L+\xi) + \frac{1}{4} \{ \exp[-2\beta(L+\xi)] + \exp[-2\beta(L-\xi)] \\
 &\quad - 2 \exp[2\beta\xi] \}], \quad -L \leq \xi < 0.
 \end{aligned} \tag{A.42}$$

We are primarily interested in the first and second moments of η . Recall:

$$E\{\rho^2\} = R_{\eta}(0) \tag{A.43}$$

$$E^2\{\rho\} = R_{\eta}(\infty)$$

$$E\{(\rho - \bar{\rho})^2\} = R_{\eta}(0) - R_{\eta}(\infty)$$

Hence

$$E^2\{\eta\} = B^2 \left(\frac{\beta s_0}{2}\right)^2 L^2 = B^2 E^2\{k^2\} L^2 \tag{A.44}$$

$$\begin{aligned}
 E\{(\eta - \bar{\eta})^2\} &= A^2 s_0 \left[L + \frac{1}{\beta} \{ \exp(-\beta L) - 1 \} \right] \\
 &\quad + B^2 \frac{s_0^2 \beta}{2} \left[L + \frac{1}{2\beta} \{ \exp(-2\beta L) - 1 \} \right].
 \end{aligned} \tag{A.45}$$

Note that

$$\lim_{\beta L \rightarrow 0} E\{(\eta - \bar{\eta})^2\} = 0 \tag{A.46}$$

and

$$E\{(\eta - \bar{\eta})^2\} \leq L [A^2 s_0 + B^2 s_0^2 \beta / 2]. \tag{A.47}$$

We therefore simplify Equation A.45 to

$$E\{(\eta - \bar{\eta})^2\} \approx L\{A^2 s_o + \frac{1}{2} B^2 s_o^2 \beta\} \quad (\text{A.48})$$

provided that $(\beta L) \gg 1$.

We may now compare terms. From Equation (3.16), Equation (A.11), and Equation (A.12), we have

$$\frac{A}{B} \approx 2K_B \quad (\text{A.49})$$

Now observe

$$\frac{2A^2 s_o}{B^2 s_o^2 \beta} = 4K_B^2 \left(\frac{2}{\beta s_o}\right) = 4K_B^2 / E\{k_r^2\} = 4/\sigma^2 \gg 1. \quad (\text{A.50})$$

Thus

$$E\{(\eta - \bar{\eta})^2\} \approx A^2 L s_o. \quad (\text{A.51})$$